Master of Environmental Engineering

Adsorption Characteristics of Modified Magnetic Coffee Waste for Removal of Tetracycline from Water

The Graduate School
of the University of Ulsan

Department of Civil and Environmental Engineering
Guohua Sun

Adsorption Characteristics of Modified Magnetic Coffee Waste for Removal of Tetracycline from Water

Supervisor: Hung-Suck Park

A Dissertation

Submitted to
The Graduate School of the University of Ulsan in Partial Fulfillment of the Requirements for the Degree of

Master of Environmental Engineering

by

Guohua Sun

Department of Civil and Environmental Engineering
University of Ulsan, Korea
July 2020

Adsorption Characteristics of Modified Magnetic Coffee Waste for Removal of Tetracycline from Water

This certifies that the thesis

of Guohua Sun is approved

Byeong-Kyu Lee

Committee Chair

Committee Member

Committee Member

Department of Civil and Environmental Engineering

University of Ulsan, South Korea

July 2020

ABSTRACT

Tetracycline (TC) is applied in many areas as a broad-spectrum antibiotic. However, TC is hardly absorbed by organisms. Most of them released and can increase the resistance of bacteria. In this point of view, plenty of TC usage will make much burden to the water environment. Therefore, it requires removal from water.

In this work, the coffee waste (CW) was used as an adsorbent to remove TC from water. The CW was modified by depositing a layer of magnetic iron oxide to synthesize magnetic coffee waste (M-CW). The characterization of CW and M-CW was performed using a scanning electron microscopy (SEM), energy dispersive X-ray spectroscopy (EDS), x-ray diffraction (XRD), thermogravimetric analysis (TGA) and Fourier Transform Infrared Spectroscopy (FT-IR). The batch adsorption experiments were conducted to investigate the effect of pH, adsorbent dosage, TC concentration, and time on adsorption. Furthermore, the mechanism of adsorption was studied by kinetics (zero-order, pseudo-first order, pseudo-second order, Elovich, and intra-particle diffusion) and isotherms (Langmuir, Freundlich, Temkin, and Dubinin-Radushkevich). Also, the response surface methodology (RSM) was employed to model and optimize the combined effect of factors on TC removal using M-CW. The empirical model was developed, statistically established through analysis of variance (ANOVA), and experimentally verified to represent adsorption of TC on M-CW. The model was adopted to identify optimum removal conditions to remove TC from water.

The characterization work shows that iron oxide (35 w/w %) was successfully deposited on M-CW. The batch experiments showed that the TC is removed best at weak acidic to neutral conditions (pH: 5-7). M-CW dosage at 0.25g/L, the TC adsorption capacity up to 127mg/g. After 56hours, the adsorption process reaches equilibrium. The experiment data fitted Pseudo-second order, Elovich, and the Langmuir model well. The theoretical maximum TC uptake capacity can be up to 102 mg/g, as calculated using the Langmuir model. It was observed that over 95% TC can be removed by M-CW at optimized conditions using RSM. This study may facilitate further investigations into the application of using waste material to remove micropollutants from water.

Keywords: Tetracycline antibiotic; adsorption; coffee waste; equilibrium; kinetics.

ACKNOWLEDGEMENTS

Many people helped me in this thesis work. I want to give sincere gratitude to their kindness and intelligence.

At first, I want to express my thanks to the professors in the Department of Civil and Environmental Engineering. They taught me a lot during the whole master course. They are so kind, patient and of course full of knowledge.

Secondly, I am very thankful to my advisor Professor Hung-Suck Park who provides the opportunity to study in his laboratory. He kindly supported me in financial, spirit motivation, and academic guidance during the whole master course.

Here I want to say thanks to Dr. Qammer Zaib. He is really smart and gives me the proper guidance in my thesis work. His positive motivation helped me get through a hard time. Without his kindness, I think it is impossible to complete this thesis work in time.

Then I want to express my greatness to my laboratory members. They always provide kind help when I get trouble in daily life and always make the laboratory like a big warm home. We take a class and discuss it together. It is so nice and lucky for me to be one of you.

Last but not least, I am very grateful to my family and friends. Your kind and positive encouragement help me to complete the thesis. Thanks to my parents with their selfless love, thanks to my husband with always patience accompanies and thank my dear friends with kind encouragement.

TABLE OF CONTENTS

LIST OF FIGURES

LIST OF TABLES

1. INTRODUCTION

1.1 Background

The antibiotic is extensively used in human and animal health treatment [1]. Among the antibiotic species, the tetracycline (TC) as a broad-spectrum antibiotic is applied in many areas [2]. It is useful in human therapy and veterinary because of its good effect on microbial infection [3]. Besides, the low price of TC interested itself to be one of the most popular antibiotics in application [4]. However, the large quantity of utilization of TC caused the problem to the environment, especially in aquatic conditions. After usage, the TC can enter the water environment through urine, feces, and manure from humans and animals [2, 3]. The fate and transport of TC is shown in Fig. 1.1 (antibiotics) [5]. Moreover, TC can hardly be biodegraded, and the residual TC might increase the antibiotic resistance of bacteria, thereby making an overall negative impact on both ecology and human health [6]. Hence, water pollution caused by TC is getting more concerns nowadays.

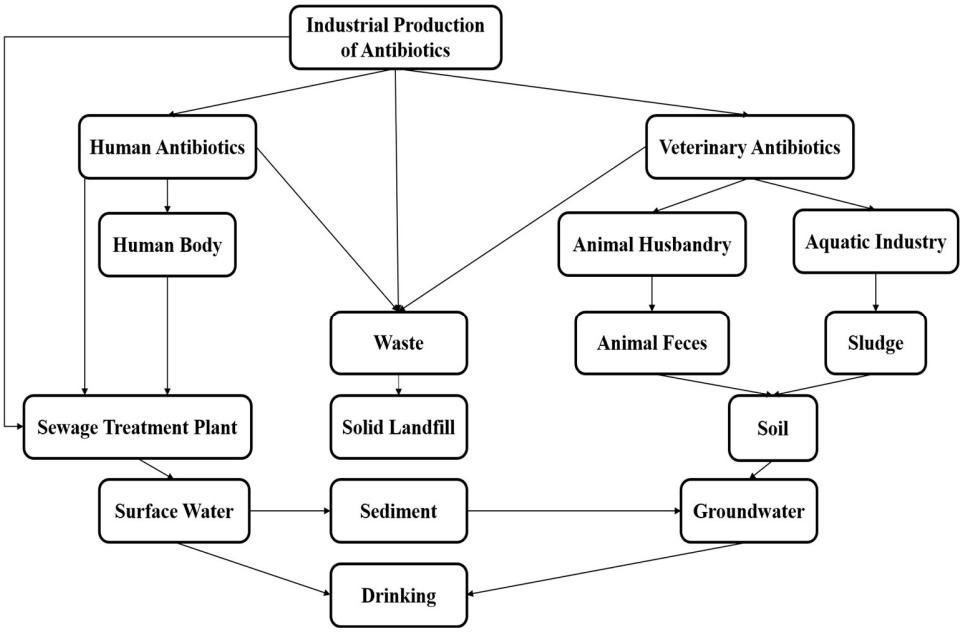

Figure 1.1: Migration of antibiotics.

There are many approaches for the removal of TC from the aquatic environment [2]. For example, membrane process [7], electrochemical process [8], photocatalytic process [9], and the adsorption process [10], etc. Among these methods, the adsorption process exhibits the advantage such as relatively low cost and high removal efficiency [3, 10]. Besides, the adsorption process is preferred because of its easy operation and virtually no secondary pollution [11, 12]. Many researchers have used various adsorbents to

remove TC. Activated carbon [13-15], different kinds of biochar [10, 12, 16], agricultural waste [11, 17], and other materials [3, 18] were used to eliminate TC in the environment. Among them, adsorbent made from agricultural or industrial waste gain much interest in recent years.

Coffee is one of the most popular drinks in the world. According to the international coffee organization (ICO), the estimated coffee consumption was over 10 million tons (169, 337,000 bags of 60 kg each) [19]. It indicates that there will produce plenty of coffee waste after coffee extraction all over the world. It was reported 1 ton of green coffee will produce about 650 kg of spent coffee ground [20, 21]. Although coffee waste is utilized in many areas, a lot of it is discarded as waste [11]. The coffee waste can be used as a resource to adsorb micropollutants, such as TC, from water [22]. Yingjie Dai et al. used two different kinds of spent coffee grounds to eliminate the TC form water [11]. And Van-Truc Nguyen et al. utilized biochar derived from spent coffee ground to remove TC [16].

Once the adsorbent is successfully used to remove the targeted contaminant from water, its recovery from the aqueous system is usually an energy-intensive and economically burdensome problem. This issue can be addressed by modifying the surface of adsorbents using magnetic materials [23, 24]. The magnetic modification can be easily operated through co-precipitation. After that, the adsorbent will be separated by the external magnetic field[25]. Therefore, the magnetic modification method has been extensively used in many areas including pollutants removal from water [26]. However, there is no study about using modified magnetic coffee waste to remove TC in wastewater reported before.

As the water pollution caused by antibiotics such as TC is getting more concerns nowadays, economically feasible removal technologies and strategies to clean water are highly desirable. This study is to repurpose and valorize the huge coffee waste to remove TC in water. Thus, the objectives of this study are: (1) to prepare and characterize magnetic coffee waste(M-CW) adsorbent, (2) to investigate the adsorption behavior of TC on the M-CW as a function of pH, M-CW dosage, TC concentration and time (3) to estimate adsorption mechanism by performing adsorption kinetics and equilibrium study. Also, a response surface methodology (RSM) was employed to comprehend the effect of the individual and combined effect of parameters on the adsorption removal process. The whole work is briefly depicted in Fig 1.2.

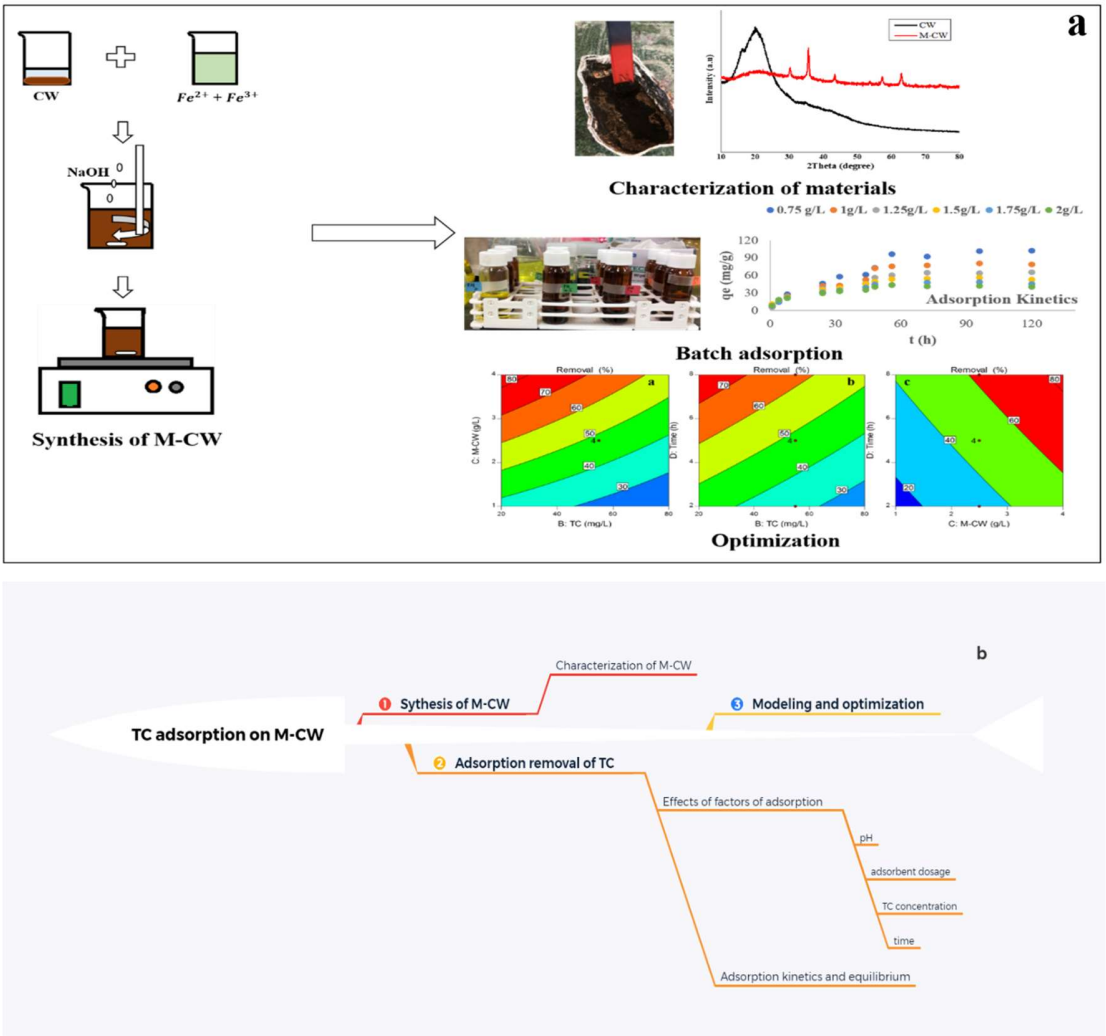

Figure 1.2: Graphic introduction of the overall study (a) and a brief flow of the whole study (b).

1.2 Objectives

The main purpose of this study is to remove the tetracycline efficiently and economically from the aqueous environment. Among the other approaches, the adsorption method has already presented a relatively good performance and low cost. There is a lot of research on activated carbon prepared from agricultural waste[17]. These activated carbons performed well in several kinds of pollutant adsorption. However, the process also increases the cost. There still need other ways to make low-cost adsorbent. Thus, this research focuses on the economic process to make the adsorbent to remove the tetracycline. This study makes the adsorbent from the spent coffee ground which considered as waste with easy and low-cost modification method. The adsorption mechanism is studied through kinetic and isotherm research. Furthermore, the optimization method is utilized to get the optimum adsorption condition.

The main objective of this thesis research is an attempt to develop an economic, good adsorption performance and easily separable adsorbent by using a magnetic modification method then investigate the TC removal efficiency capacities. For this purpose, here conclude three main parts:

1) To make an inexpensive adsorbent and test its adsorption removal capacity.
   (1) Developing a suitable method to get the target adsorbent from agriculture waste.

   (2) Characterizing adsorbent using tools such as FT-IR (Fourier Transform Infrared Spectroscopy), SEM (Scanning electron microscope), EDS (Energy-dispersive X-ray spectroscopy), XRD (X-ray diffraction), TGA (Thermogravimetric Analysis) method.
2) To study the main factors that affect the adsorption process and the mechanism of adsorption.
   (1) Performing adsorption experiments.
   (2) Kinetics and isotherms studies will be carried out for the adsorption study.
3) To find the optimum adsorption conditions by response surface methodology.

1.3 Thesis Outline and Organization

This thesis completed through a specified template and requirements for a master's degree in Environmental Engineering from the School of Civil and Environmental Engineering at the University of Ulsan, Republic of Korea.

Chapter 2 is mainly focused on the literature review of TC removal by the adsorption process. The adsorption process is reviewed in general. The adsorption removal of TC using various adsorbents, in recent years, are evaluated in detail.

Chapter 3 describes materials and methods. This part contains the material synthesis method and its characteristic detection (SEM, EDS, FT-IR, TGA, XRD, and point of zero charges). It also includes the batch experiment and optimization of the adsorption process. Moreover, the mechanism study and their theoretical models are introduced in this chapter.

Chapter 4 is the results and discussion. In this chapter, the synthesized materials and their characterization are discussed with respect to literature. The adsorption of TC on M-CW is analyzed and discussed with reference to established literature. The effects of parameters on adsorption are investigated and modeled. The adsorption mechanism is proposed and the optimum conditions for the adsorption removal of TC from water are assessed.

2. TETRACYCLINE ADSORPTION REMOVAL BY DIFFERENT ADSORBENT USING ADSORPTION METHOD

TC is a widely used antibiotic and makes burdens on the environment especially in aquatic conditions. Many researchers tried different treatment methods to eliminate TC from the aquatic systems. Among different kinds of treatments, adsorption is preferred because of its easy operation and low probability of generating secondary pollutants. In adsorption, the selection of adsorbent is critically important. The type of adsorbent exhibit different pore size, surface area, and surface chemistry and other factors that can affect the adsorption removal efficiency, adsorption mechanism, and the cost of the whole process. The sludges, activated carbons, soils and clays, chitosan, nanotubes, and composites are commonly used adsorbent in the TC adsorption process [27].

2.1 Sludges

The massively produced sludges from wastewater treatment plants usually considered industrial waste. However, proper treatment and application can make sludges to be useful material. Groundwater treatment sludge recycled to be a magnetic adsorbent by a one-step hydrothermal method with NaOH solution [28, 29]. The ferrihydrite-rich groundwater treatment sludge reused through the hydrothermal method by adding Na_2S for preparing nano-rod erdite particles applied in TC adsorption [30]. The sewage sludge was used to prepare iron-loaded biochar by one-step modification hydrothermal method and through this method, the new adsorbent enhances its surface functional groups and surface area which is helpful in TC removal [31]. Aerobic granular sludge biochar was modified by $ZnCl_2$ to produce more effective adsorbent in TC removal [32].

pH, as the most important factor, the effect in adsorption was analyzed in these studies. The change of main TC speciation in different pH conditions combined with adsorbent`s point of zero charges, the optimum pH value was varying from the different adsorbent. Normally, the removal efficiency of TC is higher in acidic conditions than basic conditions. It means most of TC in cationic and zwitterionic form was removed by these sludge derived adsorbents[28, 30].

The kinetics and isotherms were also done for the mechanism of adsorption. Most of these studies fitted well with Pseudo-second order and Langmuir isotherms[31]. It indicates chemisorption will be dominant. integrating with the pH effect, the existed adsorption mechanism can be concluded by hydrogen bonding interactions, π - π electron donor-acceptor (π - π EDA) interactions, complexation, cationic exchange, and electrostatic interaction [29, 31, 32].

2.2 Activated Carbons

Activated carbon has a strong adsorption affinity than other adsorbents [33]. And the activated carbon derived from agriculture waste gets more focused nowadays. Sugar cane bagasse modified with $ZnCl_2$ activated carbon-based adsorbent exhibit 239.6mg/g TC adsorption capacity [33]. Durian shell-based activated carbon was prepared by a physical activation method with CO_2 as an activating agent [34]. Through one-step phosphoric acid low-temperature activation, corn straw turns to activated carbon to remove TC, the TC uptake capacity reaches 227.3mg/g [35]. Apricot nutshell activated carbon synthesized by using the phosphoric acid chemical activation method [36].

The dosage of adsorbents affects adsorption performance. Because higher dosage can provide more active sites for TC molecule, the removal efficiency significantly increased with the increase of adsorbent dosage at the beginning, then slowly increased and finally remain in a relatively constant value. And the TC uptake capacity was still decreased with the increase of dosage. This phenomenon happened with the overlapping of adsorbent then decrease the adsorption efficiency of the active site [35].

Scientific characterization was conducted to get a clearer understanding of these synthesized adsorbents. This characterization involved adsorbent morphology, surface area, pore size, surface function group, and other information. After activation, the surface of activated carbon was significantly damaged and show lots of cavities by SEM image [36]. Through the surface functional group of activated carbon analysis, there exist OH, COOH, C-O, C=C, and C=O stretching vibration [33, 35, 37]. And these findings can be used in adsorption mechanism explanation like hydrogen bonding and π - π EDA interaction happened between the adsorbent surface and TC molecules. The OH and CH_3 in TC molecular can be a H acceptor interacted with oxygen-containing function groups in activated carbon [36]. TC and these adsorbents both have an aromatic ring containing π bonds can be proof of π - π EDA interaction mechanism [33]. the Activated carbon is reported to have variable surface area depending upon source material and activation processes such as $307.6 m^2/g$ [36], $463.89 m^2/g$ [35], and $831 m^2/g$ [33]. The high surface area corresponds to a higher number of active sites to remove TC.

Besides kinetics and isotherms, the thermodynamic study also takes a role in these adsorption processes. Under different temperatures, the TC adoption performance changed, and the calculated value of △G, △H, and △S provide adsorption behavior. It is found that the adsorption is endothermic and spontaneous in some adsorption process [35-37].

2.3 Soils and Clays

The soil samples with different types, 63 agricultural plots from Spain and lateritic soil, paddy soil, purplish soil, cultivated loessal soil, cinnamon soil, and black soil from a different province in China, were

collected to check the TC removal efficiency [38, 39]. It is reported that soil organic matter is the main factor in TC removal. where abundant soil component, the removal efficiency of TC was much higher than those low organic matter content soil [40]. And the pH of soil and cation exchange capacity also take an important role in TC adsorption on soils [39].

Montmorillonite and red earth clay combined with municipal solid waste was used to make biochar in the TC adsorption process [41]. Spent bleaching earth and its pyrolyzed materials used to treat TC in aqueous conditions [42]. They analyzed the effect of coexisting cations in TC removal. It is found that the different affinity of adsorbents, make the cations exhibit different strength competitive influence in TC adsorption process [42].

2.4 Chitosan

Chitosan is considered as a natural polymer. It contains a lot of functional groups and can be combined with different materials to synthesis new adsorbent [43, 44]. A waste sludge-based biochar was modified by chitosan and Fe/S to remove TC, and this modification helped the wasted sludge-based biochar improve the TC uptake capacity from 51.78mg/g to 183.01mg/g [43]. Chitosan was incorporated with metal-organic frameworks(MOFs) to adsorb TC and this operation not only improve the performance of TC adsorption but also help MOFs shape into beads [45]. The chitosan-olive pomace adsorbing films was made to remove TC and analyzed the reuse of adsorbent [46].

It is reported that the removal of TC is negatively affected by the presence of salts in solution. The monovalent and divalent cation effect was studied. The co-existing cations can hinder the electrostatic interaction between adsorbent and TC by competing with TC molecules with the surface-active site of adsorbent [45]. Furthermore, the monovalent cations may affect the adsorption performance through enhance screen effect of adsorbent surface charges to reduce the affinity and the divalent cation may form a cation-TC complex to inhibit the interaction of adsorbent and TC [46].

2.5 Carbon Nanotubes

According to the high specific surface area, hollow, and layered structures, the carbon nanotubes have been considered as potential superior adsorbents [47, 48]. A multi-walled carbon nanotube deposited iron metal-organic framework composite was used to remove TC and the characterization work shows this kind of combination enhances the specific surface area, pore-volume, and thermal stability of the new adsorbent [49]. Heteroatom nitrogen-doped multiwall carbon nanotube was synthesized to treat TC in solution [48]. The alumina-coated multi-walled carbon nanotube was made for TC adsorption [47].

The initial concentration of TC can affect the adsorption behavior. The high concentration provides the driving forces and lets TC molecules move to the adsorption site which can be helpful in TC uptake

capacity improvement [50]. However, the removal percentage may decrease with the increase of initial concentration. The same dosage adsorbent can be saturated after a certain amount of TC molecules, and then no more adsorption can occur [47].

2.6 Composites

A different variety of composites were used as adsorbent. The TC-imprinted composite cryogel was made for selective TC adsorption [51]. The different ratios of oil palm ash and electric arc furnace steel slag were used to make mesoporous zeolite-hydroxyapatite-activated palm ash composites to adsorb TC [50]. The magnetic carbon-α Fe/Fe_3C adsorbent was synthesized by the carbonization method and this method significantly improve the specific surface area and pore volume then highly increase the adsorption capacity of TC in aqueous condition [52].

The removal efficiency of TC by different materials was concluded by the following table 2-1

Table 2-1: removal efficiency of TC by different materials.

Materials	Treatment	TC Removal efficiency (%) / capacity (mg/g)	references
Groundwater treatment sludge	a one-step hydrothermal method with NaOH solution	362.3 mg/g	[28]
groundwater treatment sludge	hydrothermal method by adding Na_2S	1960.8 mg/g	[30]
Sewage sludge	one-step modification hydrothermal method	104.86 mg/g	[31]
Aerobic granular sludge	$ZnCl_2$ modification method	93.44 mg/g	[32]
Sugar cane bagasse	activation method with $ZnCl_2$	239.6 mg/g	[33]
Durian shell	physical activation method with CO_2	126.08 mg/g	[34]
Corn straw	one-step phosphoric acid low-temperature activation method	227.3 mg/g	[35]
Apricot nutshell	phosphoric acid chemical activation method	308.33 mg/g	[36]
Soil from Spain	-	>58%	[38]
Spent bleaching earth	pyrolysis process	85.4%	[42]
Waste sludge-based biochar	modified by chitosan and Fe/S	183.01 mg/g	[43]
Metal-organic frameworks (MOFs)	incorporated with chitosan	495.04 mg/g	[45]
Multi-walled carbon nanotube	alumina-coating method	876.8 mg/g	[47]
Magnetic carbon- α Fe/Fe_3C	carbonization method	511.06 mg/g	[52]

3. MATERIALS AND METHODS

3.1 Materials and reagents

TC (≥ 98%) used as a target pollutant was purchased from Sigma-Aldrich, MO., USA. Ferric chloride hexahydrate ($FeCl_3.6H_20$) (≥ 98%) and ferrous sulfate ($FeSO_4.7H_2O$) (≥ 98.5%) were acquired from Sigma-Aldrich, MO., USA and Junsei Chemical Co., Ltd., Japan, respectively. Sodium Hydroxide (NaOH) (≥ 98%) and sodium chloride (NaCl) (≥ 99.5%) were purchased from OCI Company Ltd., South Korea. Hydrochloride acid (HCl) (≥36%) was supplied by Daejung Chemicals & Metals Co., Ltd., South Korea. Distilled deionized water was used in all experiments.

3.2 Synthesis of M-CW

The CW was collected from a coffee shop near Ulsan University, Ulsan, Korea. It was washed with distilled water several times, then dried in an oven at 80℃ for 24 hours. The dried CW was stored in a sealed container for later use.

The M-CW was synthesized as follows: (1) 5g CW was added to 50ml distilled water. (2) 5 g FeCl3.6H2O and 2.75 g $FeSO_4.7H_2O$ were put into 150ml distilled water to make the iron solution. (3) After thoroughly dissolved, the iron solution was put into CW suspension and mixed 30 minutes using magnetic stirrer [53, 54]. In this period, 5M NaOH was made for making iron precipitation. (4) After mixing, the suspension was added 5M NaOH dropwise until the pH of supernatant reach 11. (5) The suspension was then heated at 95℃ using hotplate stirrer (MSH-20D) for 1 hour and cooled to room temperature before filtering. (6) The precipitation was washed by distilled water several times until the pH of supernatant remained constant. (7) And the material was dried at 80℃ in the oven for 24hours. Finally, the synthesized M-CW material was stored in a sealed container for later use. A brief synthesis procedure of M-CW was depicted in Fig. 3.1.

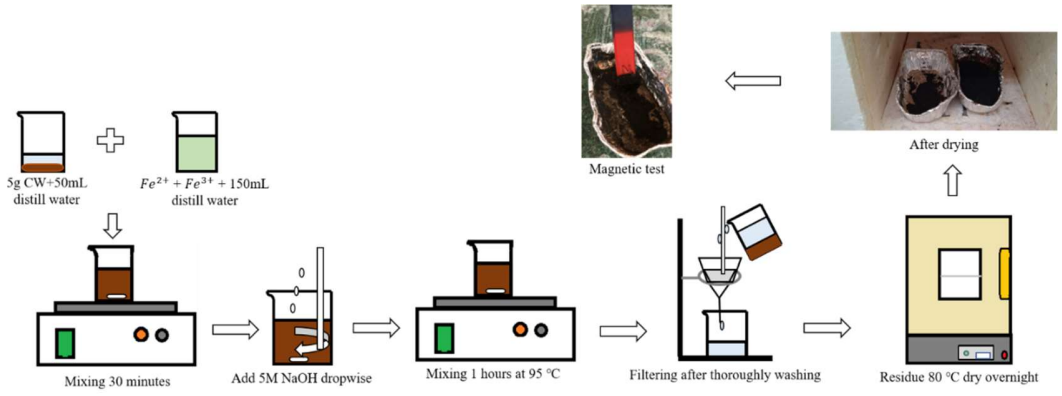

Figure 3.1: M-CW synthesis procedure

3.3 Physio-chemical characterization of CW and M-CW materials

The characterization was performed using tools like FT-IR, SEM, EDS, XRD, TGA method. Field Emission Scanning electron microscope (FE-SEM) JSM-6500 was from JEOL, Japan. It was operated at 15kV for the morphology study of the CW and M-CW. Energy dispersive X-ray spectroscopy (EDS) associated with the FE-SEM machine was used to determine the elemental composition of two materials. The material function group analysis was carried by Fourier Transform Infrared Spectroscopy (FT-IR) Nicolet iS5 from Thermo Fisher Scientific, USA. Differential Scanning Calorimeter-Thermogravimetric analyzer (DSC-TGA) SDT Q600 was from TA, USA. This one was used to do the weight loss analysis in the air conditioner by the increasing temperature at 5°C/min rate until 600°C. X-Ray Diffractometer (XRD) Ultima IV from Rigaku, Japan conducted the materials crystal structural analysis.

The point of zero charge (pH_{pzc}) was determined [14, 55, 56] by the following steps. (1) 0.01M NaCl solution was made and divided into 9 different flasks. (2) The pH was adjusted by 1M and 0.1M NaOH and 1M and 0.1M HCl from 2 to 10. (3) 20mL of adjusted NaCl solutions were taken and put into several 20ml glass bottle with 0.02g materials (CW and M-CW) respectively. (4) After two days of mixing, the final pH was detected. The difference between the initial pH and the final pH was monitored. Change in pH (△pH) provided the estimate of isoelectric point (pH_{pzc}) of the samples.

3.4 Batch adsorption experiments

Batch adsorption experiments were conducted to investigate the removal efficiency of TC by M-CW. The stock solution of 500 mg/L TC was made for the following experiments. 1M and 0.1M NaOH and HCl were used for adjusting the pH of solutions. And different factors (pH, M-CW dosage, time) were selected for the adsorption experiment. In adsorption experiments, the TC solution pH ranged from 2-11, the adsorbent dosage from 0.25g/L - 2g/L, and adsorption time from 1-120 hours. For the pH effect experiment, the pH 2,5,7,9 and 11 were selected and the experiment time set as 25hours. It was conducted at 150rpm incubator shaker (iNtRON Biotechnology, Korea) with the initial concentration of TC at 100mg/L, M-CW dosage at 1g/L, and temperature at 25°C. This study also conducts the effect of dosage in the adsorption process. The M-CW dosage selected 0.25,0.75,1,1.25,1.5,1.75,2g/L, TC initial concentration 100mg/L, pH 5, temperature 25°C, agitation 150rpm and time 56hours.

The TC concentration was analyzed by DR 2800 Spectrophotometers (HACH, USA). The detection wavelength was selected as 355nm [16]. The calibration curve was made against the different concentrations of TC and the correlation coefficient R^2>0.99.

The TC removal efficiency (R%) was calculated through the following Eq. (1).

$$R\% = \frac{(C_0 - C_e)}{C_0} \times 100 \quad (1)$$

C_0(mg/L) is the initial concentration of TC and C_e(mg/L) is the concentration of TC when the adsorption reaches equilibrium.

3.5 Adsorption mechanism: kinetic and isotherms

The adsorption kinetics and isotherms of TC on the M-CW were performed at constant temperature and pressure. The stock solution of TC was diluted to 100 mg/L and pH 5 was adjusted using 1M HCl and 1M NaOH for kinetics and isotherm study. The adsorption experiment was carried at 25℃, 150rpm incubator shaker. The different time 1,4,8,24,32,44,48,56,72,96,120 hours were selected, and the dosage of M-CW is constant at 1.5g/L for doing adsorption kinetics. The dosages of M-CW were 0.75,1,1.25,1.5,1.75,2g/L and 56 hours were used for equilibrium study. The TC uptake capacity on M-CW was calculated by Eq. (2). and Eq. (3).

$$q_e = \frac{(C_0 - C_e)V}{m} \tag{2}$$

$$q_t = \frac{(C_0 - C_t)V}{m} \tag{3}$$

q_e(mg/g) represents the adsorption capacity at equilibrium condition, q_t(mg/g) represent the adsorption capacity at any time of t, C_t(mg/L) is the concentration of TC at any time of t in the solution, V(L) is the volume of solution and m(g) is the dosage of the adsorbent.

The adsorption kinetics data was evaluated using zero-order, pseudo-first-order, pseudo-second-order, Elovich, and Intra-particle diffusion models [57]. Here concluded their non-linear and linear form equations.

The zero-order.

$$q_t = q_e - k_0 t \tag{3.4}$$

Where k_0 (mg/(g•h)) is the zero-order kinetic model constant

The Pseudo-first order

$$q_t = q_e(1 - \exp(k_1 t)) \tag{3.5}$$

$$\log(q_e - q_t) = \log q_e - (\frac{k_1}{2.303})t \tag{3.6}$$

k_1 (h^{-1}) is the constant of Pseudo-first order

The Pseudo-second order

$$q_t = \frac{k_2\, q_e^2\, t}{1+ k_2\, q_e\, t} \tag{3.7}$$

$$\frac{t}{q_t} = \frac{1}{k_2 q_e^2} + \frac{1}{q_e} t \tag{3.8}$$

Where k_2 (g/(mg•h)) is the Pseudo-second order rate constant

The Elovich

$$q_t = \beta \ln(\alpha\beta t) \tag{3.9}$$

$$q_t = \beta \ln(\alpha\beta) + \beta lnt \tag{3.10}$$

Where α ((mg/(g•h)) is the initial adsorption rate and β (g/mg) is the desorption constant.

The intraparticle diffusion

$$q_t = K_i t^{1/2} \tag{3.11}$$

K_i (mg/ (g• $h^{0.5}$)) is the intraparticle diffusion rate constant

The Langmuir, Freundlich, Temkin, and Dubinin–Radushkevich (D–R) isotherm model [58, 59] were selected to model the adsorption data. Their non-linear and linear form equation are given below:

The Langmuir isotherm equation

$$q_e = \frac{Q_{max} K_L\, C_e}{1+K_L C_e} \tag{3.12}$$

$$\frac{C_e}{q_e} = \frac{1}{K_L Q_{max}} + \frac{C_e}{Q_{max}} \tag{3.13}$$

There is another parameter R_L in Langmuir isotherm called separation factor used to determine the type of isotherm [60]. Normally, R_L=0 indicates irreversible adsorption, 0<R_L<1 means favorable, R_L=1 is linear and R_L>1demonstrate unfavorable. The R_L calculated by Eq. (3.14)

$$R_L = \frac{1}{1+K_L C_0} \tag{3.14}$$

Where, C_e (mg/L) is the TC adsorption equilibrium concentration, Q_{max} (mg/g) is the maximum TC uptake capacity on monolayer, K_L (mg/g) is the Langmuir isotherm constant and R_L is the dimensionless separation factor.

The Freundlich isotherm

$$q_e = K_F {C_e}^{1/n} \tag{3.15}$$

$$log\ q_e\ = log\ K_F + \frac{1}{n} log\ C_e \tag{3.16}$$

Where K_F ((mg/g) •(L/mg)$^{1/n}$) is the Freundlich isotherm constant and n is adsorption intensity. The 1/n can be an indicator in this isotherm. When 1/n<1 means a normal Langmuir isotherm and if 1/n>1 indicates cooperative adsorption [60].

The Temkin isotherm

$$q_e = \frac{RT}{b} \ln(AC_e) \tag{3.17}$$

$$q_e = \frac{RT}{b} lnA + \frac{RT}{b} lnC_e \tag{3.18}$$

Where A (L/g) is the Temkin isotherm equilibrium binding constant, b is the Temkin isotherm constant, R (8.314 J/mol•K) is the universal gas constant and T (K) is the temperature. There is a constant related to the heat of sorption B in Temkin isotherm. Its unit is J/mol and the equation like the following.

$$B = \frac{RT}{b} \tag{3.19}$$

The Dubinin-Radushkevich isotherm

$$q_e = (q_s) \exp(-K_{DR}\, \varepsilon^2) \tag{3.20}$$

$$q_e = (q_s) \exp(-K_{DR}\, \varepsilon^2) \tag{3.21}$$

Where

$$\varepsilon = RT \ln\left(1 + \frac{1}{C_e}\right) \tag{3.22}$$

Where q_s (mg/g) is theoretical isotherm saturation capacity, K_{DR} (mol^2/KJ^2) is the Dubinin-Radushkevich isotherm constant and Ɛ is the Dubinin–Radushkevich isotherm constant. With the value of K_{DR}, it can calculate the mean free energy E (kJ/mol) which can indicate whether the process is chemisorption or physisorption[61]. The Eq. (3.23) shows the relationship of K_{DR} and E. when the value of E range from 8-16 KJ/mol indicates chemisorption and below to 8 means physisorption [62].

$$E = \frac{1}{\sqrt{2K_{DR}}} \tag{3.23}$$

The best-fitted model was selected through R^2 which indicates the model fitting degree and root mean sum-of-squares error (RMSE) determination test. the small RMSE value means the similarity of experimental and calculated values [58, 63]. The RMSE equation like followings

$$RMSE = \sqrt{\frac{\sum_1^N (qe,cal - q\ ,\exp)^2}{N}} \tag{3.24}$$

Where, $q_{e,exp}$ (mg/ g) is the experimental sorption capacity, $q_{e,cal}$ (mg/g) is the model calculated (predicted) sorption capacity and N is the number of experimental points.

3.6 Optimization study

Generally, a one-factor-at-a-time (OFAT) parametric study is often conducted in research work [64]. This kind of study can sufficiently describe the adsorption mechanism. However, the OFAT method cannot account for the interactions between different parameters. Thus, it is necessary to use an optimization method to conduct a more comprehensive research.

RSM was selected to design an experiment for optimization in this study. As a statistical method, RSM can provide a more efficient and economic experimental design. Furthermore, it can be used in the study of the interaction of experimental factors [18]. There are several experimental design methods in RSM. Among them, the central composite design method (CCD) was taken to obtain the experimental design matrix. Many researchers used CCD for their experimental design [65, 66]. Four independent variables were chosen in this study. They are pH (A), TC initial concentration mg/L (B), M-CW dosage g/L (C) and contact time h (D). Each of them has five levels and detailed information was concluded in Table 3-1.

Table 3-1: Experimental factors and their levels for the removal of tetracycline using M-CW.

	Factors	**Units**	**Levels**				
			−α	***-1***	***0***	***1***	***+α***
A	pH	-	3	5	7	9	11
B	Tetracycline	mg/L	10	33	55	77	100
C	M-CW	g/L	0	1.25	2.5	3.75	5
D	Time	h	2	3.5	5	6.5	8

TC adsorption removal efficiency was used to be the response of this adsorption study and Analysis of Variance (ANOVA) conducted to judge the statistical significance of the model.

4. RESULTS AND DISCUSSION

4.1 Synthesis of M-CW

The M-CW synthesis method is following simply modified chemical precipitation [53]. The $FeCl_3.6H_2O$ and $FeSO_4.7H_2O$ solution provide nearly 1:2 M ratio of Fe^{2+} and Fe^{3+} ions[54]. At the presence of precipitating agent NaOH solution, the material experience following steps.

$$FeCl_3 \rightarrow Fe^{3+} + 3Cl^- \tag{4.1}$$

$$FeSO_4 \rightarrow Fe^{2+} + SO_4^{2-} \tag{4.2}$$

$$2Fe^{3+} + Fe^{2+} + 8OH^- \rightarrow Fe_3O_4 + 4H_2O \tag{4.3}$$

Fig. 4.1 shows the phenomena before and after magnetic separation works on the M-CW. It indicates the M-CW can be easily separated by a magnetic bar. And the modification results whether Fe_3O_4 coated on M-CW or not will get through the characterization works.

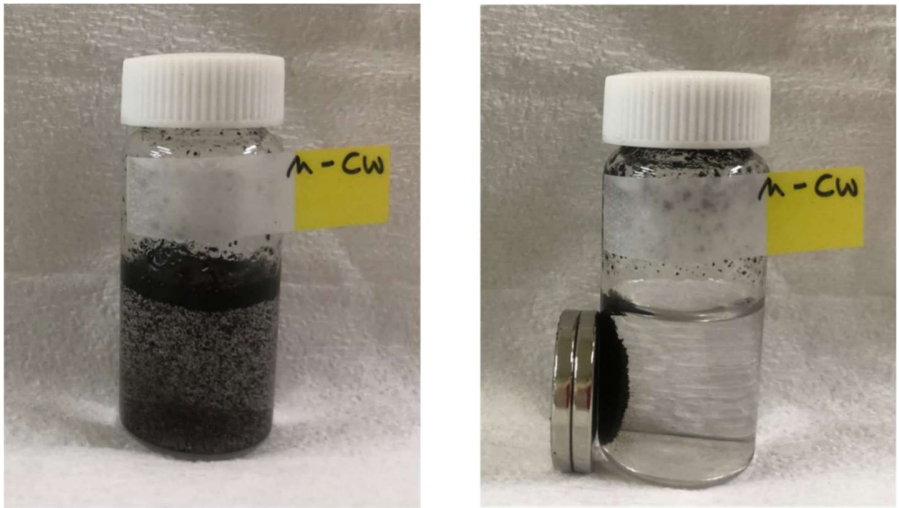

Figure 4.1: M-CW before and after magnetic separation

4.2 Characterization

4.2.1 Surface morphology analysis of M-CW

The high-magnification SEM image about CW and M-CW was depicted in Fig.4.2. It shows the difference between CW and M-CW surfaces clearly. Comparing with the smooth surface of CW, M-CW has a much rougher surface.

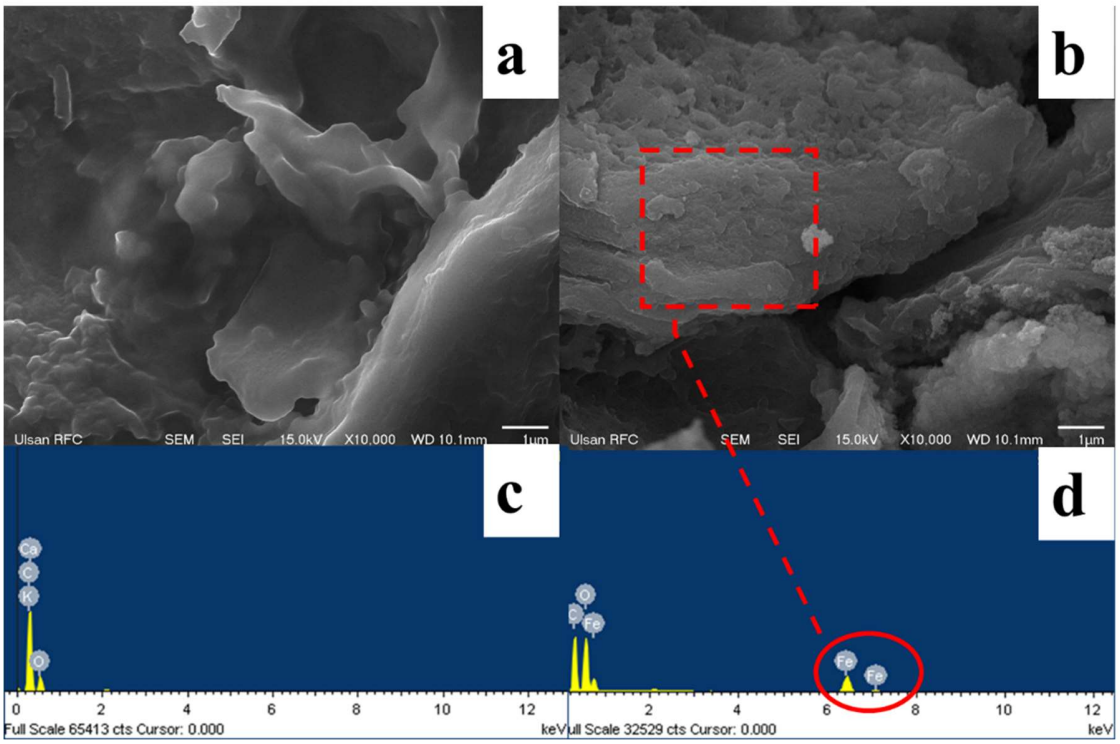

Figure 4.2: SEM micrograph of CW(a) and M-CW(b) EDS spectrum of CW(c) and M-CW(d)

This difference can be explained by the EDS analysis. Carbon and oxygen are the main constituents of CW. However, the main composition is changed to carbon, oxygen, and iron in M-CW. The element content in CW and M-CW concluded in Table 4-1.

Table 4-1: Element content analysis by EDS for M-CW and CW

M-CW			CW		
Element	Weight%	Atomic%	Element	Weight%	Atomic%
C	43.50	57.23	C	74.91	79.97
O	38.00	37.54	O	24.91	19.96
Fe	18.50	5.24	Mg	0.05	0.03
-	-	-	K	0.07	0.02
-	-	-	Ca	0.06	0.02
Totals	100.00		Totals	100.00	

This observation can tell the successful deposition of iron oxides on M-CW. The deposition of iron oxides makes the M-CW surface rougher than CW. Similar surface roughness is observed by other researchers [23, 53]. The rough surface is helpful in the adsorption process because it may enhance the specific surface area.

4.2.2 The FT-IR analysis of M-CW

FT-IR can tell the function groups existed in the surface area of the material. In order to get further confirmation of iron oxides existence in M-CW, FT-IR analysis was done, and the result shown in Fig. 4.3. There can be found characteristic peaks at 1060 cm^{-1} both CW and M-CW which originated from C-O-C stretching caused by chlorogenic acids existed in coffee [53]. The peaks appear at 1740 cm^{-1}, are caused by C=O stretching and at 2920 cm^{-1} peaks is attributed to C-H stretching existed in cellulose [16, 53]. The 2850 cm^{-1} and 3320 cm^{-1} are ascribed COOH stretching and O-H stretching [67]. Upon iron treatment, the new stretch at 558 cm^{-1} appeared in M-CW compared with CW. The new peaks can be assigned to the presence of Fe-O stretching vibration [67, 68]. This finding can be strong proof about the iron oxides successfully coated on the surface of M-CW.

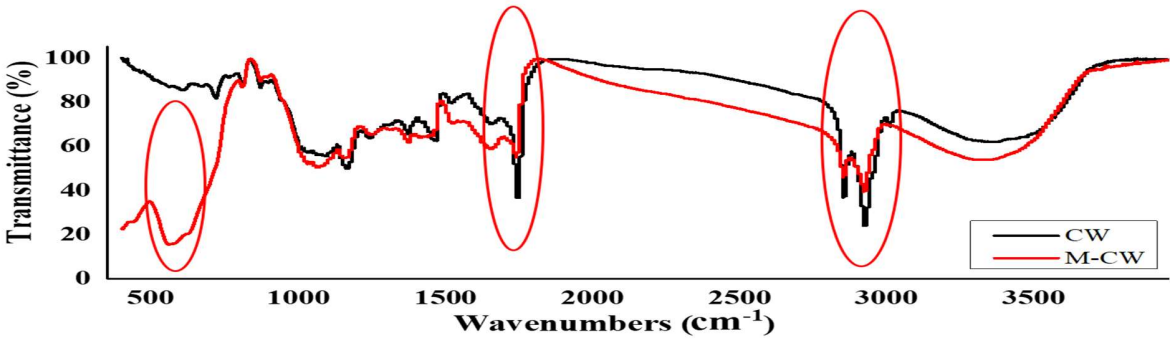

Figure 4.3: FT-IR spectra of CW and M-CW

4.2.3 Thermogravimetric analysis of CW and M-CW

The thermogravimetric analyses of CW and M-CW were shown in Fig. 4.4. It reflects the thermal stability of two materials and with comparison can roughly show the content of iron oxides coated in M-CW. The mass was slightly decreased before 250℃, it can be the reason for some moisture volatilization in both materials. And then the mass was sharply decreased until maintain to constant. This means materials keep stable in the third stage. Finally, the CW loss of 96.53% of the mass and M-CW loss of 60.93% of the mass. With a combination of the results getting from SEM-EDS and FT-IR analysis, the 35% mass loss difference between CW and M-CW mainly caused by the existence of iron oxides deposited in M-CW.

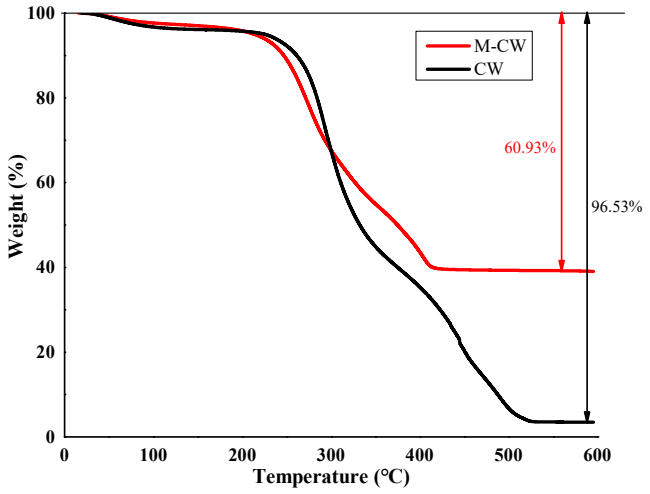

Figure 4.4: Thermogravimetric analysis of CW and M-CW

4.2.4 XRD results of CW and M-CW

To understand the speciation of iron oxides existed in M-CW, XRD analysis was conducted. The XRD pattern of CW and M-CW were depicted in Fig.4.5. There are two broad peaks in 16.22° and 20.06° at CW which indicates the presence of lignocellulose structure [69]. The sharp and intense peaks appearing at 30.25°, 35.56°, 43.33°, 57.22°, and 62.84° at 2 Theta value in M-CW. This indicates the presence of Fe_3O_4 in the surface of coffee waste without altering their crystal structure [53, 67, 70, 71]

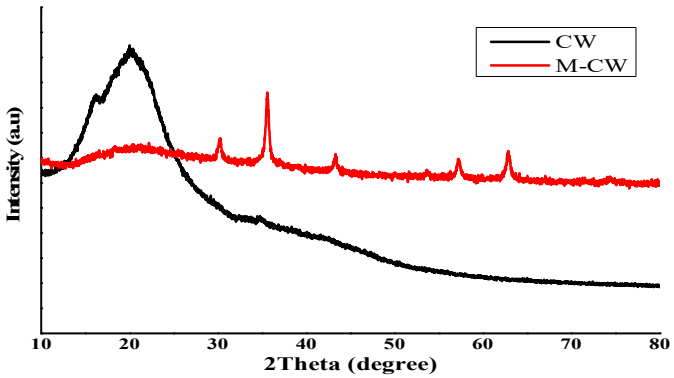

Figure 4.5: XRD pattern of CW and M-CW

4.2.5 Point of zero charge (pH_{pzc}) of CW and M-CW

pH takes an important role in the adsorption process. In this view of point, the pH_{pzc} of adsorbent gives important information in the whole adsorption work. It provides a different surface charge of adsorbent in different pH value solution. The pH_{pzc} of two materials (CW and M-CW) were shown in Fig.4.6. The pH_{pzc} about CW is 4.8 and M-CW is 4.4. It indicates the pH of solution lower than 4.4, the surface charge of M-CW will be positive and on the contrary pH > 4.4, the surface of M-CW turns to negatively charged.

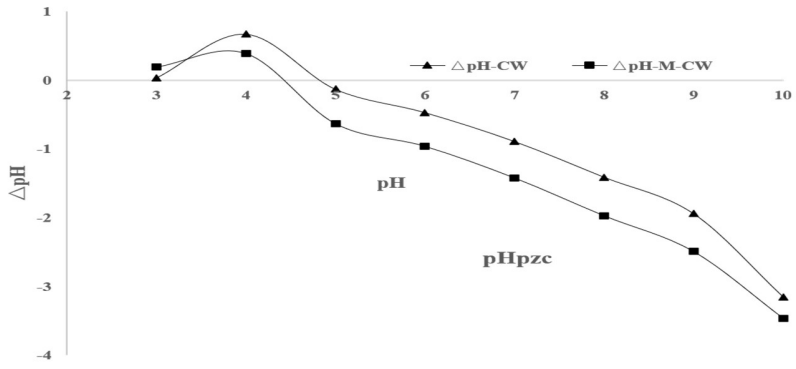

Figure 4.6: pH_{pzc} of CW and M-CW

4.3 pH and dosage effect on adsorption

4.3.1 pH effect on adsorption

TC have stayed in different ionic species in different pH value [16, 72]. More detailed information about TC can be seen in Table 4-2 [11]. Since pH can change the surface charge of the adsorbent. According to the change of material surface charge at different pH values, it can affect the electrostatic adsorption between adsorbate and adsorbent [11].

Table 4-2: TC detailed information

CAS:	**60-54-8**
Chemical structure	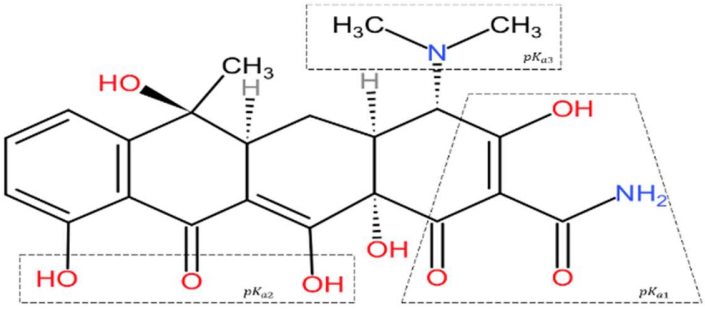
Chemical formula	$C_{22}H_{24}N_2O_8 \bullet xH_2O$
Molar mass	444.43 g/mol
pKa$_1$	3.3
pKa$_2$	7.7
pKa$_3$	9.7

The effect of pH on TC removed by M-CW is shown in Fig. 4.7. It shows in the low pH value, the removal of TC is around 40%. It can be explained that in low pH values like pH equal to 2 the most speciation of TC is the cationic form (TCH_3^+) and the M-CW surface is positively charged [3]. Because of electrostatic repulsion, the removal efficiency of TC might be not high. This can also explain the high pH value. pH >4.4 the surface charge of M-CW is negative, and when the pH > 7.7 most of TC exists in anion form (TCH^- or TC^{2-}) [17]. In this case, electrostatic repulsion makes resistance between adsorbate and adsorbent. However the removal of TC still exists, it is may cause by the intermolecular π-π interactions or hydrogen bonding between TC molecule and M-CW surface [3, 14]. When the solution pH between 4.4 and 7.7 M-CW exhibits pretty good TC removal performance. The reason is M-CW stay in negative charged and most of TC remain in zwitterionic condition in this pH range. With the Fig. 4.7 it can be concluded the TC removed better in the weak acidic environment.

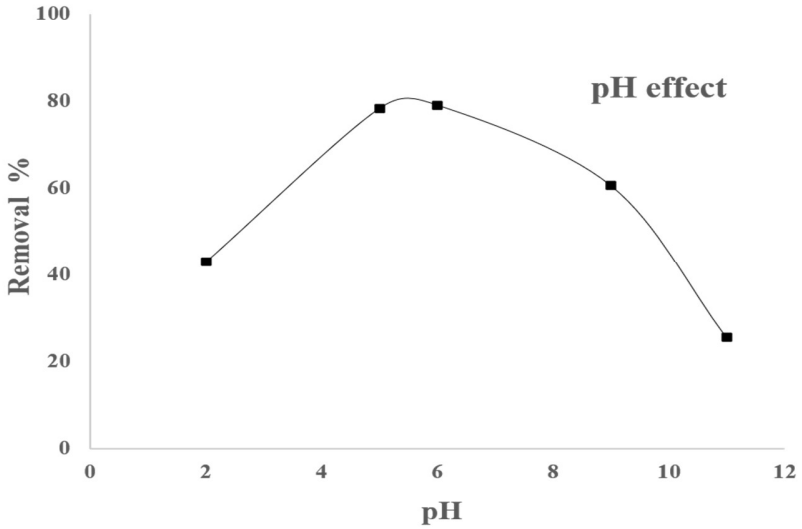

Figure 4.7: pH effect in the adsorption process. experiment condition: TC initial concentration 100mg/L, M-CW dosage 1g/L, pH 2-11, temperature 25°C, time 25 h, agitation 150rpm

4.3.2 Dosage effect on adsorption

To understand the effect of adsorbent dosage in the adsorption process, different dosages of M-CW were prepared to adsorb 100mg/L TC solution and the process was described by Fig. 4.8. The TC uptake capacity was different from 43-127 mg/g with the difference of M-CW dosages. The removal efficiency increased sharply with the increase of adsorbent dose up to 1g/L then slowly increased. In a constant TC concentration(100ppm), the increase of the M-CW dosage provides more active sites for adsorption. However, too much increase of adsorbent is not increasing the removal efficiency significantly. This can be explained by adsorbent overlapping of the active sites [67].

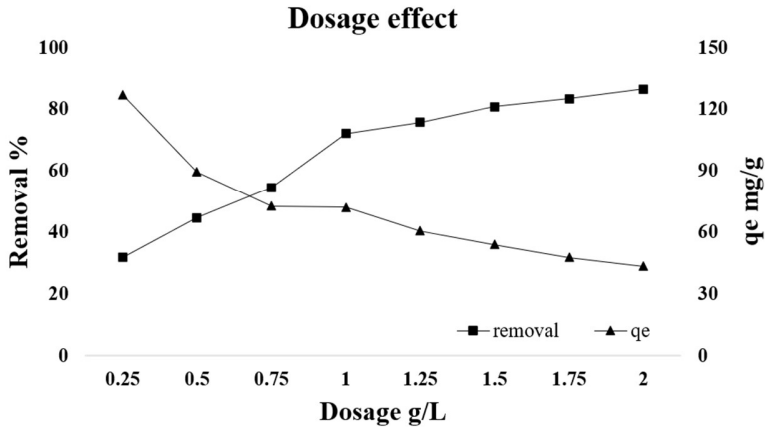

Figure 4.8: Dosage effect on adsorption. experiment condition: TC initial concentration 100mg/L, M-CW dosage 0.25-2g/L, pH 5, temperature 25°C, time 56 h, agitation 150rpm

4.4 Adsorption kinetics

The adsorption process experiences mass transfer, diffusion(external and pore diffusion), and surface reaction [63, 73]. Each one can provide resistance to influence the rate of getting adsorption equilibrium. Adsorption kinetics study is useful to find out the equilibrium time, TC uptake rate-limiting factors, and provide the main resistance existed in the adsorption process. Fig. 4.9 depicts the kinetic plot with different dosages of the adsorbent. With this figure, the TC adsorption process reaches equilibrium around 56hours.

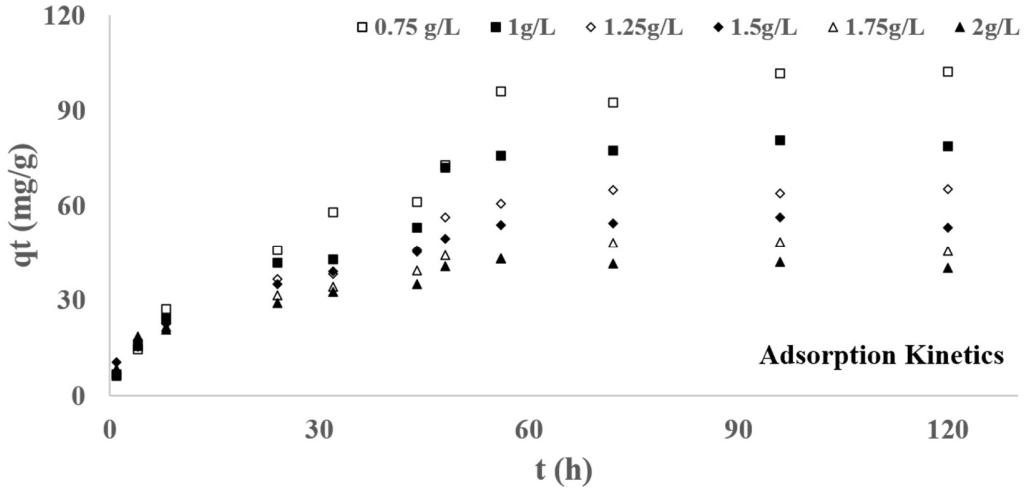

Figure 4.9: Adsorption kinetic plot in different M-CW dosage. Experimental conditions: TC initial concentration 100ppm, pH 5.0, agitation speed 150 rpm, temperature 25 °C, adsorbent dosage 0.75-2g/L time 1, 4, 8, 24, 32, 44, 48, 56, 72, 96 , 120 hours.

The empirical models can be helpful to study the adsorption kinetics. This study selected five models to explain the adsorption process. The linear plot of these models can be shown in Fig. 4.10 and the model parameters are shown in Table 4-3.

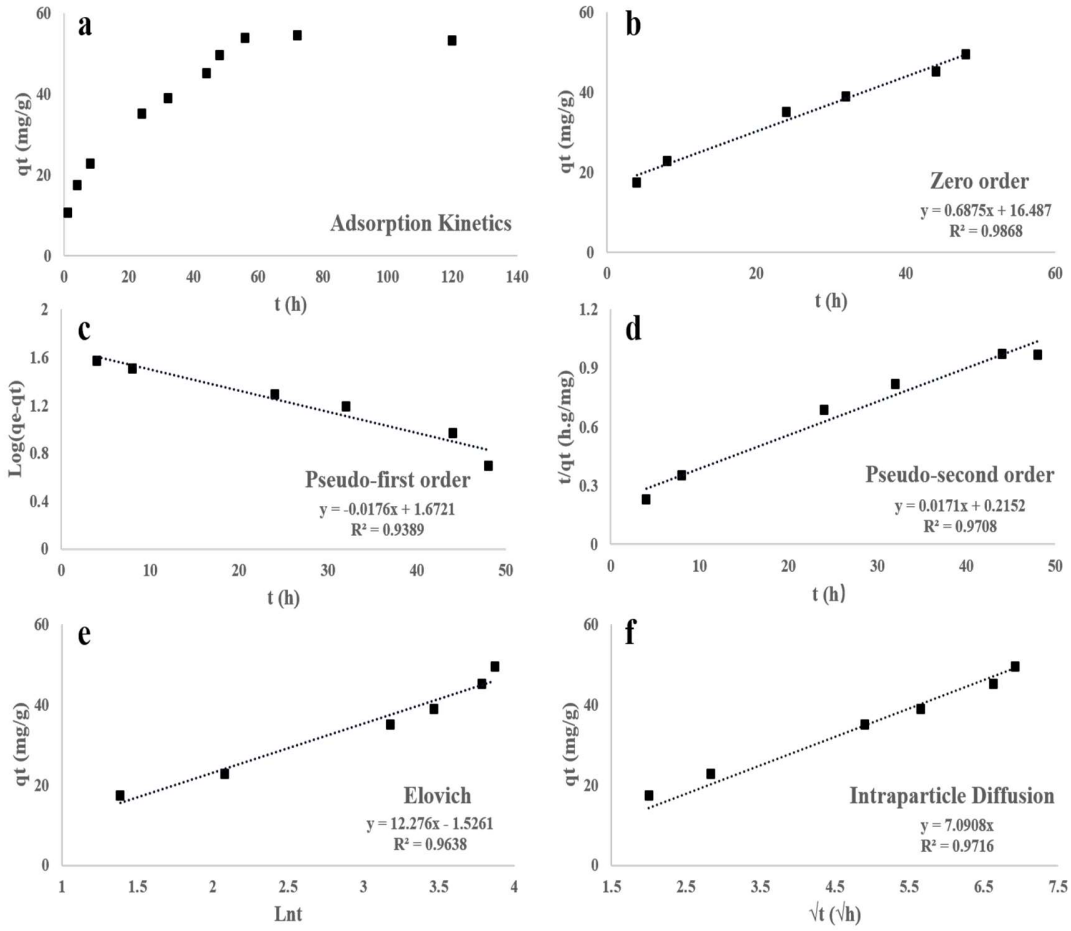

Figure 4.10: Adsorption kinetic plot(a) and different kinetic models linear plot about TC adsorption on M-CW(b-f).

One of the adsorption kinetics plots among several different dosages of M-CW kinetic data (M-CW dosage: 1.5g/L) was shown in Fig. 4.10. a. The linear plot of Zero-order kinetics is in Fig. 4. 10 b. The R2 equal to 0.9868 is higher than other kinetic models, however, the RMSE value shown in Table 4-3 is the highest one. It means zero order model is not fitted well in this adsorption process.

Table 4-3: Adsorption kinetics constant in TC adsorption removal process

Zero order	
q_e mg/g	16.487
k_0 mg/(g•h)	-0.6875
R^2	0.9868
RMSE	38.02
Pseudo-first order model	
Calculated qe mg/g	47.000
Experimental qe mg/g	54.51
k_1 (h^{-1})	0.041
R^2	0.9389
RMSE	7.51
Pseudo-second order model	
Calculated qe mg/g	58.479
k_2 (mg/g•h)	0.001
R^2	0.9708
RMSE	3.97
Elovich	
α mg/(g•h)	0.072
β g/mg	12.276
R^2	0.9638
RMSE	3.53
Intraparticle diffusion	
K_i mg/(g•$h^{0.5}$)	7.0908
R^2	0.9716
RMSE	5.66

Pseudo-first order equation and Pseudo-second order are widely used in adsorption kinetic research. They are fitted well in most of the adsorption process. Both the R^2 values are relatively high and RMSE values are small. It means these reactions limiting factor models fitted well in the TC adsorption process. Comparing the R^2 and RMSE value, Pseudo-second order model fit the experimental data better.

Elovich model also reflects chemisorption that existed in the adsorbate-adsorbent system. The R^2 and RMSE value shows this model also fit well in this study. And the lowest RMSE value means the calculated TC uptake capacity is the closest to the experimental data. The value of R^2 and RMSE Intraparticle diffusion model exhibit this model also fit the experimental data well. And it can be the explanation of long equilibrium time consumes in this adsorption process. However, it can hardly get through the origin. It indicates the intraparticle diffusion is not the only limiting factor in the adsorption process.

Because of the high agitation speed and small particle size, the effect of mass transfer can be mostly reduced [63]. Above all, it can be concluded TC adsorbed on the M-CW process contains two main resistance. One from the surface reaction and the other from intraparticle diffusion.

4.5 Adsorption isotherms

The adsorption isotherm can tell the mechanism of the adsorption process. Here some experiential models will help learn adsorption isotherm. The equilibrium data fitted by four isotherms in this study. The linear plots and some important parameters in isotherm study were concluded by Fig. 4. 11 and Table 4-4.

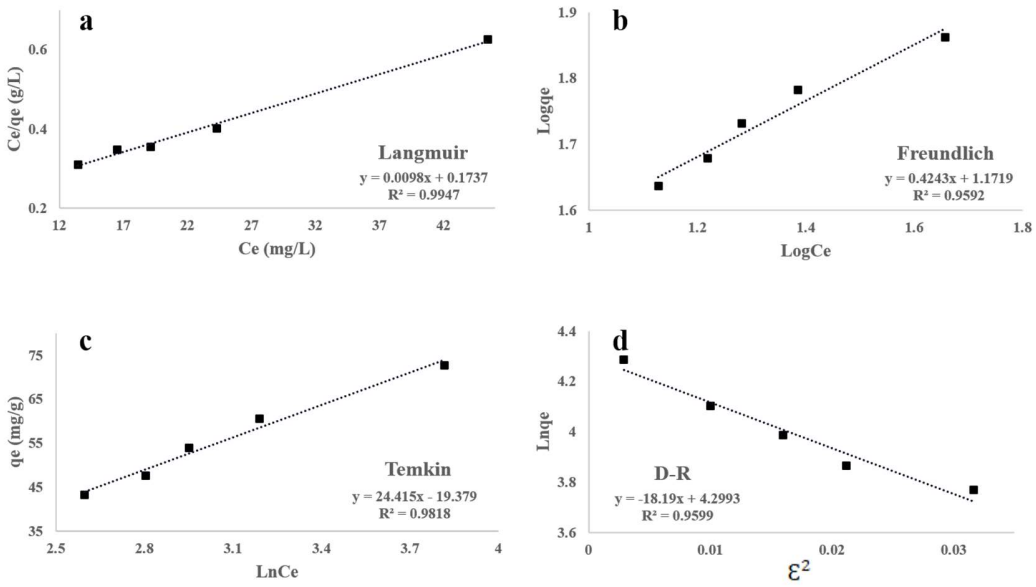

Figure 4.11: Adsorption isotherms linear plot of TC adsorption on M-CW

The Langmuir isotherm assumes monolayer adsorption on the homogeneous adsorbent surface [60]. The linear plot of the Langmuir equation is shown in Fig. 4. 11. a. The parameters were calculated with the slope and intercept of the plot and they are shown in Table 4-4. The calculated data, it shows the maximum uptake capacity of TC on the M-CW is 102 mg/g and the RMSE value indicates there exists a small difference between experimental and calculated data. By comparison with other adsorbents, the TC uptake capacity of M-CW performs well, and the results can be seen in Table 4-5. Besides, the obtained constant R_L here is 0.024 between 0 and 1, this range of value reflects TC adsorption on the M-CW is a favorable process [58]. This all means the Langmuir model is fitted well in this study.

Table 4-4: Adsorption isotherms constant in TC adsorption removal process

Langmuir	
K_L L/mg	0.056
Qmax mg/g	102.041
R_L	0.152
R^2	0.9947
RMSE	1.18
Freundlich	
K_F (mg/g) (L/mg)1/n	14.856
n	2.357
R^2	0.9592
RMSE	2.11
Temkin	
A (L/g),	0.452
B (J/mol)	24.415
R^2	0.9818
RMSE	1.39
Dubinin–Radushkevich	
K_{DR} mol^2/kJ^2	18.19
q_s mg/g	73.648
E kJ/mol	0.166
R^2	0.9599
RMSE	1.97

The Freundlich equation is an empirical model that assumes the adsorption took place in heterogeneous systems. And the intensity n value can describe some possibility. The Freundlich linear plot was shown in Fig. 4. 11. (b). According to the slop and intercept calculate the parameters then concluded in Table 4-4. 1/n value here is $0<0.4243<1$, it indicates a normal Langmuir isotherm fitted in this study [60].

Temkin isotherm usually used to describe the interaction between adsorbent and adsorbate. There is an assumption that the adsorption heat has a linear variation with the degree of overlap [74]. With the coefficient concluded in Table 4-4, the R^2 is 0.9818 and the constant related to the heat of adsorption is 24.415J/mol which indicates physisorption [74].

D-R isotherm model as an empirical model was applied to describe the adsorption mechanism about Gaussian energy distribution onto a heterogeneous surface [58]. And the value of E can be used to distinguish chemisorption or physisorption occurred in the system. When the E value lower than 8 kJ/mol it means physisorption or between 8-16 kJ/mol the procedure may chemisorption [62]. The linear plot of D-R isotherm can be seen in Fig. 4. 11. d. and Table 4-4 concluded the mean values. The R^2 is 0.9599 and the E value is 0.166 kJ/mol which can be considered physisorption occurred in this adsorption system.

The comparable R^2 value and RMSE value shows Langmuir isotherm fitted best in this study. It means the TC adsorbed in a relatively favorable homogeneous surface. The Temkin and D-R isotherm

models can be proof of physisorption existence in the whole adsorption process. This means the Van der Waals may play a role in this adsorption process.

Table 4-5: Comparison of the maximum adsorption capacities of TC onto various adsorbents based on Langmuir isotherms.

Adsorbents	pH	Adsorbent dosage (g/L)	Equilibrium time (h)	Q_{max} (mg/g) Langmuir	References
Fe HAP	5	1	6	41.39	[75]
Rice straw biochar	-	1	24	50.72	[72]
Rice husk ash	5	2	10	8.37	[17]
Bamboo charcoal	7	1	24	22.7	[76]
M-CW	5	0.5	56	102.04	This study
Porous carbon material	-	1	27	210.18	[13]
MOF-5	7	0.3	1	233	[3]
Sulfonated tea waste	-	0.5	0.5	416.66	[77]

4.6 Adsorption optimization study

The four factors and both experimental and model-predicted response results concluded in Table 4-6.

Table 4-6: Experimental design matrix and response of experimental settings for the adsorption removal of TC by M-CW.

Run	Factors				Response	
	A: pH	**B:** Tetracycline (mg/L)	**C:** M-CW (g/L)	**D:** Time (h)	Tetracycline adsorption removal (%)	
					Experimental	Predicted
1	7	10	2.5	5	65.4	64.48
2	3	55	2.5	5	37.3	37.99
3	5	77	3.75	6.5	70.5	65.51
4	9	77	3.75	3.5	33.9	31.51
5	9	77	1.25	6.5	23.8	15.97
6	5	77	1.25	6.5	29.9	28.93
7	5	77	3.75	3.5	48	44.47
8	7	55	2.5	2	27	32.79
9	7	55	2.5	8	59.3	62.73
10	11	55	2.5	5	0	12.07
11	7	55	5	5	75.9	81.36
12	5	33	1.25	3.5	27.2	27.72
13	7	55	2.5	5	46.5	47.76
14	9	33	1.25	3.5	23.4	14.75
15	9	33	3.75	6.5	74.8	68.24
16	7	100	2.5	5	28.1	31.04
17	5	33	3.75	3.5	69.1	70.24
18	7	55	2.5	5	45.4	47.76
19	9	33	1.25	6.5	35.6	35.56
20	5	77	1.25	3.5	25.3	21.87
21	5	33	3.75	6.5	77.4	81.21
22	7	55	2.5	5	48.4	47.76
23	9	77	3.75	6.5	52.3	52.55
24	7	55	0	5	0.5	14.16
25	7	55	2.5	5	42.7	47.76
26	9	77	1.25	3.5	15.5	8.91
27	9	33	3.75	3.5	62.4	57.27
28	5	33	1.25	6.5	55.4	48.52

The relationship equation between variables and response as following equation Eq. (4.4):

Tetracycline Removal (%) = 47.7605 - 6.48147A - 8.36047B + 16.798C + 7.48364D -2.00272BC - 0.459747BD + 0.518598CD - 5.68291A2 + 2.9769BCD (4.4)

The positive part in this equation means the corresponding factor increased and the response can be improved. The same meaning with the negative part.

The experimental data against the model predicted value plot was depicted in Fig. 4. 12. Some of the data is in the predicted value line and the other is uniformly separated both sides of the line. It tells the model can predict well in this adsorption process. The statistical analysis of the model was studied by ANOVA.

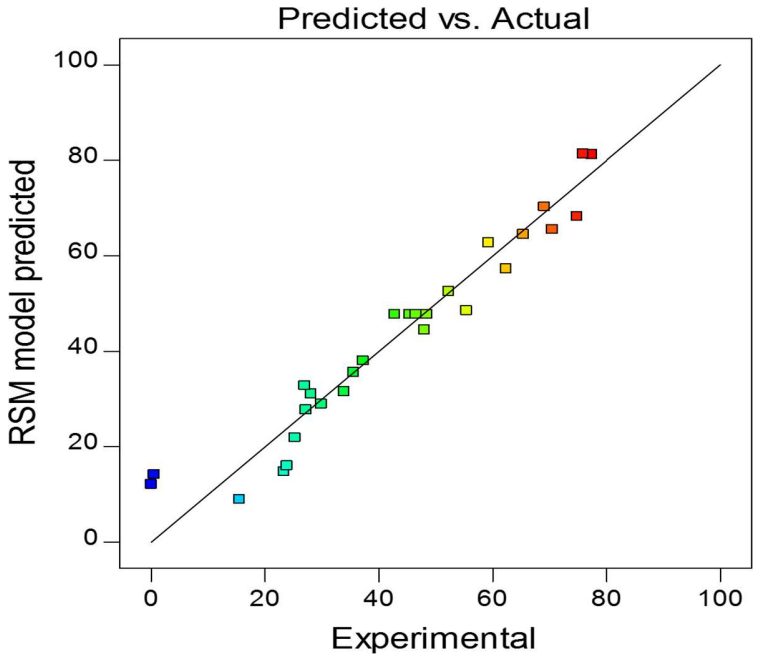

Figure 4.12: Experimental vs model-predicted response of TC adsorbed by M-CW

The ANOVA of the reduced cubic model in TC adsorption on M-CW was concluded in Table 4-7. It can be shown that the model is statistically significant at 95% confidence level. Since the p-value is less than 0.0001, meaning the significance term. The B, C, D are the most significant terms in this model. This means the significant effect of every single factor in TC removal. Even though the lake of fit is significant, the R^2 equal to 0.9357 is larger than 0.9 which means the model can predict the experiment process well[78].

Table 4-7: The analysis of variance (ANOVA) of the reduced cubic model in TC adsorption by M-CW.

ANOVA for Reduced Cubic model Removal (%) of tetracycline by M-CW						
Source	Sum of Squares	df	Mean Square	F-value	p-value	
Model	11901.53	9	1322.39	29.08	< 0.0001	significant
A-pH	1008.23	1	1008.23	22.17	0.0002	
B-TC	1677.54	1	1677.54	36.89	< 0.0001	
C-M-CW	6772.18	1	6772.18	148.93	< 0.0001	
D-Time	1344.12	1	1344.12	29.56	< 0.0001	
BC	64.17	1	64.17	1.41	0.2503	
BD	3.38	1	3.38	0.0744	0.7882	
CD	4.3	1	4.3	0.0946	0.7619	
A^2	885.82	1	885.82	19.48	0.0003	
BCD	141.79	1	141.79	3.12	0.0944	
Residual	818.49	18	45.47			
Lack of Fit	801.6	15	53.44	9.49	0.0443	
Pure Error	16.89	3	5.63			
Cor Total	12720.01	27				
Std. Dev.	6.74		R^2	0.9357		
Mean	42.89		Adjusted R^2	0.9035		
C.V. %	15.72		Predicted R^2	0.8044		
			Adeq Precision	17.977		

Fig. 4.13 shows the single factors effected in TC removal by M-CW. The pH was varied from 3-11. With the value increasing the removal efficiency slightly increased and then decreased. The phenomenon is the same as the pH value discussion part. TC concentration increased from 10 to 100 mg/L. The removal efficiency is decreased following the increase of TC concentration. It can be explained by the result of isotherm work. The adsorption process fitted the Langmuir isotherm model best, it means that the TC molecules adsorbed by M-CW surface by monolayer. With the concentration increasing, there no more surface site provided for adsorption, then the removal efficiency decreased. M-CW dosage select from 0 to 5g/L. When the dosage increased the TC removal efficiency improved significantly. Because the dosage increased then the surface activated sites used in adsorption increased. The contact time as the last factor changes from 2 to 8 hours. We can find the time factor has a positive effect on TC removal. And all these

effects can be reflected by the Eq. (4). With the combination of Fig. 4. 13, we can find the M-CW dosage has a dominant effect than other single factors.

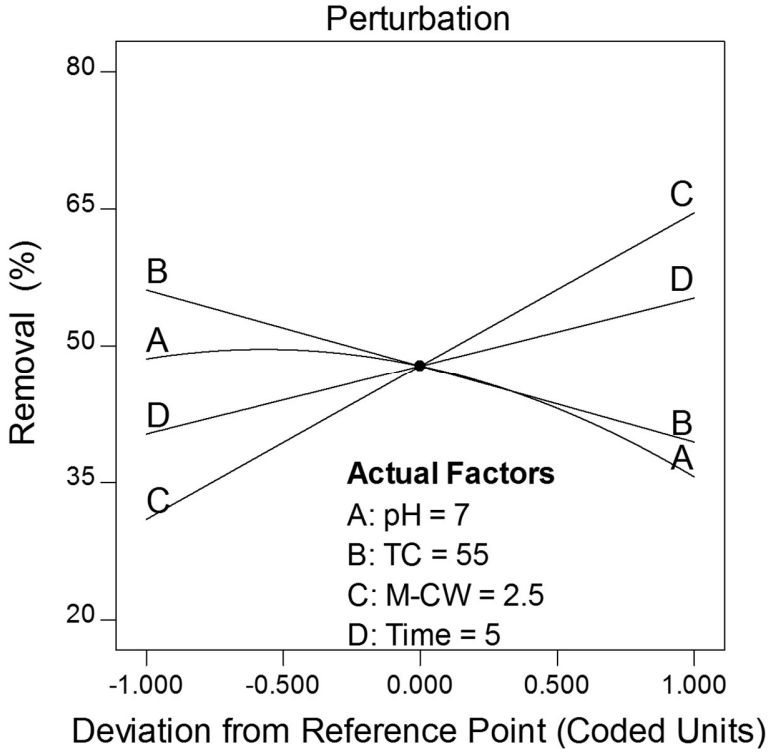

Figure 4.13: Effect of one factor on tetracycline removal

Fig. 4.14. a. shows the TC concentration and M-CW dosages combined effect in TC removal. Under constant dosage value, the removal efficiency is decreased by the increase of TC concentration. In a higher dosage compared with low dosage value, the TC concentration-effect has much more fluctuated. With low TC concentration and high M-CW dosage, the TC adsorption attach higher removal efficiency. Fig. 4. 14. b. is the TC concentration and contact time combined effect in TC removal. The concentration of TC has a negative effect on TC removal. Since in high TC concentration conditions, the TC removal is still higher than 50% at a relatively long time. Fig. 4. 14. c. depicts the TC removal changed by M-CW dosage and contact time joint effect. The M-CW dosage and contact time both are positive factors in TC removal. It means a high value of time and an M-CW dosage can contribute to high TC removal efficiency.

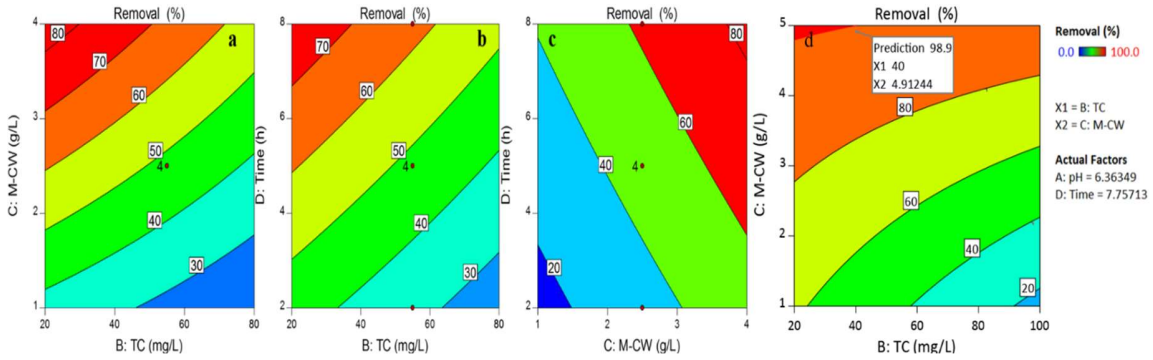

Figure 4.14: Effect of initial TC concentration and M-CW dosage on TC removal(a), Effect of initial TC concentration and time on TC removal(b) and Effect of M-CW dosage, time on tetracycline removal(c) and Predicted optimum condition for TC removal on M-CW(d)

The optimum experimental conditions to remove TC are shown in Fig. 4.14. d. The TC removal efficiency can be up to 98.9% at pH 6.4, contact time 7.7h, M-CW dosage large than 4.9 g/L, and TC initial concentration lower than 40 mg/L.

CONCLUSIONS

This study investigates the adsorption potential of agricultural waste material for the removal of tetracycline from water. The coffee waste was modified to make magnetic coffee waste (M-CW) which was utilized to adsorb and eliminate the tetracycline in the water environment. The physiochemical characterization study shows a successful modification of the adsorbent. SEM image, FT-IR functional group analysis, and XRD crystal structure study show that the presence of Fe_3O_4 on the M-CW surface. And comparing with CW, the TGA analysis quantitatively determines the 35% (w/w) presence of iron oxide in M-CW.

Three important factors, pH, M-CW dosage, and contact time, were selected to study their effect on the adsorption process. pH effect study finds that the zwitterionic form was mainly adsorbed on M-CW at weakly acidic pH value. The dosage of M-CW also influences the TC adsorption capacity. The TC removal efficiency was significantly increased with the increase of M-CW dosage $\leq$ 1g/L. The contacted time experiments showed that the TC adsorption on M-CW reaches equilibrium at 56 hours.

Adsorption kinetics and isotherms were conducted for the TC removal mechanism. The experimental data was represented by the Pseudo-second model, Elovich, and Langmuir, Temkin models well. And this indicates, there exist both chemisorption and physisorption in the process. The Langmuir isotherm fits the experimental data well and the relatively small RMSE value postulates that the adsorption phenomenon can be explained by monolayer adsorption. The maximum adsorption capacity was calculated to be 102 mg/g.

Furthermore, with the optimum study, we get the predicted model equation related to TC removal efficiency with four main factors (TC initial concentration, M-CW dosage, pH, and contact time). At pH 6.4, contact time 7.7h, M-CW 4.9 g/L, and TC initial concentration 40 mg/L, the TC removal efficiency can be 98.9%.

REFERENCE

[1] K. Kummerer, Antibiotics in the aquatic environment--a review--part I, Chemosphere 75(4) (2009) 417-34.

[2] R. Daghrir, P. Drogui, Tetracycline antibiotics in the environment: a review, Environmental Chemistry Letters 11(3) (2013) 209-227.

[3] S.M. Mirsoleimani-azizi, P. Setoodeh, S. Zeinali, M.R. Rahimpour, Tetracycline antibiotic removal from aqueous solutions by MOF-5: Adsorption isotherm, kinetic and thermodynamic studies, Journal of Environmental Chemical Engineering 6(5) (2018) 6118-6130.

[4] L. Pan, Y. Cao, J. Zang, Q. Huang, L. Wang, Y. Zhang, S. Fan, J. Tang, Z. Xie, Preparation of Iron-Loaded Granular Activated Carbon Catalyst and Its Application in Tetracycline Antibiotic Removal from Aqueous Solution, Int J Environ Res Public Health 16(13) (2019).

[5] Y. Dai, M. Liu, J. Li, S. Yang, Y. Sun, Q. Sun, W. Wang, L. Lu, K. Zhang, J. Xu, W. Zheng, Z. Hu, Y. Yang, Y. Gao, Z. Liu, A review on pollution situation and treatment methods of tetracycline in groundwater, Separation Science and Technology 55(5) (2019) 1005-1021.

[6] C. Peiris, S.R. Gunatilake, T.E. Mlsna, D. Mohan, M. Vithanage, Biochar based removal of antibiotic sulfonamides and tetracyclines in aquatic environments: A critical review, Bioresour Technol 246 (2017) 150-159.

[7] D. Zhi, J. Wang, Y. Zhou, Z. Luo, Y. Sun, Z. Wan, L. Luo, D.C.W. Tsang, D.D. Dionysiou, Development of ozonation and reactive electrochemical membrane coupled process: Enhanced tetracycline mineralization and toxicity reduction, Chemical Engineering Journal 383 (2020).

[8] M. Foroughi, A.R. Rahmani, G. Asgari, D. Nematollahi, K. Yetilmezsoy, M.R. Samarghandi, Optimization and Modeling of Tetracycline Removal from Wastewater by Three-Dimensional Electrochemical System: Application of Response Surface Methodology and Least Squares Support Vector Machine, Environmental Modeling & Assessment (2019).

[9] S. Adhikari, H.H. Lee, D.-H. Kim, Efficient visible-light induced electron-transfer in z-scheme MoO3/Ag/C3N4 for excellent photocatalytic removal of antibiotics of both ofloxacin and tetracycline, Chemical Engineering Journal (2019).

[10] Y. Zhou, Y. He, Y. He, X. Liu, B. Xu, J. Yu, C. Dai, A. Huang, Y. Pang, L. Luo, Analyses of tetracycline adsorption on alkali-acid modified magnetic biochar: Site energy distribution consideration, Sci Total Environ 650(Pt 2) (2019) 2260-2266.

[11] Y. Dai, K. Zhang, X. Meng, J. Li, X. Guan, Q. Sun, Y. Sun, W. Wang, M. Lin, M. Liu, S. Yang, Y. Chen, F. Gao, X. Zhang, Z. Liu, New use for spent coffee ground as an adsorbent for tetracycline removal in water, Chemosphere 215 (2019) 163-172.

[12] P. Zhang, Y. Li, Y. Cao, L. Han, Characteristics of tetracycline adsorption by cow manure biochar prepared at different pyrolysis temperatures, Bioresour Technol 285 (2019) 121348.

[13] M.J. Ahmed, M.A. Islam, M. Asif, B.H. Hameed, Human hair-derived high surface area porous carbon material for the adsorption isotherm and kinetics of tetracycline antibiotics, Bioresour Technol 243 (2017) 778-784.

[14] H.M. Jang, S. Yoo, Y.K. Choi, S. Park, E. Kan, Adsorption isotherm, kinetic modeling and mechanism of tetracycline on Pinus taeda-derived activated biochar, Bioresour Technol 259 (2018) 24-31.

[15] J. Rivera-Utrilla, C.V. Gomez-Pacheco, M. Sanchez-Polo, J.J. Lopez-Penalver, R. Ocampo-Perez, Tetracycline removal from water by adsorption/bioadsorption on activated carbons and sludge-derived adsorbents, J Environ Manage 131 (2013) 16-24.

[16] V.T. Nguyen, T.B. Nguyen, C.W. Chen, C.M. Hung, T.D. Vo, J.H. Chang, C.D. Dong, Influence of pyrolysis temperature on polycyclic aromatic hydrocarbons production and tetracycline adsorption behavior of biochar derived from spent coffee ground, Bioresour Technol 284 (2019) 197-203.

[17] Y. Chen, F. Wang, L. Duan, H. Yang, J. Gao, Tetracycline adsorption onto rice husk ash, an agricultural waste: Its kinetic and thermodynamic studies, Journal of Molecular Liquids 222 (2016) 487-494.

[18] M. Topal, E.I. Arslan Topal, Optimization of tetracycline removal with chitosan obtained from mussel shells using RSM, Journal of Industrial and Engineering Chemistry 84 (2020) 315-321.

[19] world coffee consumption 2020.01. http://www.ico.org/trade_statistics.asp.

[20] L. Blinová, M. Sirotiak, Utilization of Spent Coffee Grounds for Removal of Hazardous Substances from Water: A Review, Research Papers Faculty of Materials Science and Technology Slovak University of Technology 27(44) (2019) 145-152.

[21] P.S. Murthy, M. Madhava Naidu, Sustainable management of coffee industry by-products and value addition—A review, Resources, Conservation and Recycling 66 (2012) 45-58.

[22] I. Anastopoulos, M. Karamesouti, A.C. Mitropoulos, G.Z. Kyzas, A review for coffee adsorbents, Journal of Molecular Liquids 229 (2017) 555-565.

[23] B. Kakavandi, A. Takdastan, N. Jaafarzadeh, M. Azizi, A. Mirzaei, A. Azari, Application of Fe3O4@C catalyzing heterogeneous UV-Fenton system for tetracycline removal with a focus on optimization by a response surface method, Journal of Photochemistry and Photobiology A: Chemistry 314 (2016) 178-188.

[24] A.A. Atia, A.M. Donia, W.A. Al-Amrani, Adsorption/desorption behavior of acid orange 10 on magnetic silica modified with amine groups, Chemical Engineering Journal 150(1) (2009) 55-62.

[25] C. Muthukumaran, V.M. Sivakumar, M. Thirumarimurugan, Adsorption isotherms and kinetic studies of crystal violet dye removal from aqueous solution using surfactant modified magnetic nanoadsorbent, Journal of the Taiwan Institute of Chemical Engineers 63 (2016) 354-362.

[26] C.H. Yen, H.L. Lien, J.S. Chung, H.D. Yeh, Adsorption of precious metals in water by dendrimer modified magnetic nanoparticles, J Hazard Mater 322(Pt A) (2017) 215-222.

[27] S.S. Priya, K.V. Radha, A Review on the Adsorption Studies of Tetracycline onto Various Types of Adsorbents, Chemical Engineering Communications 204(8) (2017) 821-839.

[28] Z. Qu, Y. Wu, S. Zhu, Y. Yu, M. Huo, L. Zhang, J. Yang, D. Bian, Y. Wang, Green Synthesis of Magnetic Adsorbent Using Groundwater Treatment Sludge for Tetracycline Adsorption, Engineering 5(5) (2019) 880-887.

[29] S. Zhu, Y. Wu, Z. Qu, L. Zhang, Y. Yu, X. Xie, M. Huo, J. Yang, D. Bian, H. Zhang, L. Zhang, Green synthesis of magnetic sodalite sphere by using groundwater treatment sludge for tetracycline adsorption, Journal of Cleaner Production 247 (2020).

[30] Z. Qu, G. Dong, S. Zhu, Y. Yu, M. Huo, K. Xu, M. Liu, Recycling of groundwater treatment sludge to prepare nano-rod erdite particles for tetracycline adsorption, Journal of Cleaner Production 257 (2020).

[31] J. Wei, Y. Liu, J. Li, Y. Zhu, H. Yu, Y. Peng, Adsorption and co-adsorption of tetracycline and doxycycline by one-step synthesized iron loaded sludge biochar, Chemosphere 236 (2019) 124254.

[32] L. Yan, Y. Liu, Y. Zhang, S. Liu, C. Wang, W. Chen, C. Liu, Z. Chen, Y. Zhang, ZnCl2 modified biochar derived from aerobic granular sludge for developed microporosity and enhanced adsorption to tetracycline, Bioresour Technol 297 (2020) 122381.

[33] Y. Cai, L. Liu, H. Tian, Z. Yang, X. Luo, Adsorption and Desorption Performance and Mechanism of Tetracycline Hydrochloride by Activated Carbon-Based Adsorbents Derived from Sugar Cane Bagasse Activated with ZnCl2, Molecules 24(24) (2019).

[34] A. Yazidi, M. Atrous, F. Edi Soetaredjo, L. Sellaoui, S. Ismadji, A. Erto, A. Bonilla-Petriciolet, G. Luiz Dotto, A. Ben Lamine, Adsorption of amoxicillin and tetracycline on activated carbon prepared from durian shell in single and binary systems: Experimental study and modeling analysis, Chemical Engineering Journal 379 (2020).

[35] Q. Yang, P. Wu, J. Liu, S. Rehman, Z. Ahmed, B. Ruan, N. Zhu, Batch interaction of emerging tetracycline contaminant with novel phosphoric acid activated corn straw porous carbon: Adsorption rate and nature of mechanism, Environ Res 181 (2020) 108899.

[36] M.H. Marzbali, M. Esmaieli, H. Abolghasemi, M.H. Marzbali, Tetracycline adsorption by H3PO4-activated carbon produced from apricot nut shells: A batch study, Process Safety and Environmental Protection 102 (2016) 700-709.

[37] J. Zhou, F. Ma, H. Guo, Adsorption behavior of tetracycline from aqueous solution on ferroferric oxide nanoparticles assisted powdered activated carbon, Chemical Engineering Journal 384 (2020).

[38] M. Conde-Cid, D. Fernandez-Calvino, J.C. Novoa-Munoz, A. Nunez-Delgado, M.J. Fernandez-Sanjurjo, M. Arias-Estevez, E. Alvarez-Rodriguez, Experimental data and model prediction of tetracycline adsorption and desorption in agricultural soils, Environ Res 177 (2019) 108607.

[39] Y. Chen, C. Hu, D. Deng, Y. Li, L. Luo, Factors affecting sorption behaviors of tetracycline to soils: Importance of soil organic carbon, pH and Cd contamination, Ecotoxicol Environ Saf 197 (2020) 110572.

[40] M. Conde-Cid, G. Ferreira-Coelho, M. Arias-Estevez, D. Fernandez-Calvinho, A. Nunez-Delgado, E. Alvarez-Rodriguez, M.J. Fernandez-Sanjurjo, Adsorption/desorption of three tetracycline antibiotics on different soils in binary competitive systems, J Environ Manage 262 (2020) 110337.

[41] K.S.D. Premarathna, A.U. Rajapaksha, N. Adassoriya, B. Sarkar, N.M.S. Sirimuthu, A. Cooray, Y.S. Ok, M. Vithanage, Clay-biochar composites for sorptive removal of tetracycline antibiotic in aqueous media, J Environ Manage 238 (2019) 315-322.

[42] D. Wan, L. Wu, Y. Liu, J. Chen, H. Zhao, S. Xiao, Enhanced Adsorption of Aqueous Tetracycline Hydrochloride on Renewable Porous Clay-Carbon Adsorbent Derived from Spent Bleaching Earth via Pyrolysis, Langmuir 35(11) (2019) 3925-3936.

[43] J. Liu, B. Zhou, H. Zhang, J. Ma, B. Mu, W. Zhang, A novel Biochar modified by Chitosan-Fe/S for tetracycline adsorption and studies on site energy distribution, Bioresour Technol 294 (2019) 122152.

[44] J. Ma, Y. Lei, M.A. Khan, F. Wang, Y. Chu, W. Lei, M. Xia, S. Zhu, Adsorption properties, kinetics & thermodynamics of tetracycline on carboxymethyl-chitosan reformed montmorillonite, Int J Biol Macromol 124 (2019) 557-567.

[45] R. Zhao, T. Ma, S. Zhao, H. Rong, Y. Tian, G. Zhu, Uniform and stable immobilization of metal-organic frameworks into chitosan matrix for enhanced tetracycline removal from water, Chemical Engineering Journal 382 (2020).

[46] V. Rizzi, D. Lacalamita, J. Gubitosa, P. Fini, A. Petrella, R. Romita, A. Agostiano, J.A. Gabaldon, M.I. Fortea Gorbe, T. Gomez-Morte, P. Cosma, Removal of tetracycline from polluted water by chitosan-olive pomace adsorbing films, Sci Total Environ 693 (2019) 133620.

[47] D. Balarak, Y. Mahdavi, F. Mostafapour, Application of Alumina-coated Carbon Nanotubes in Removal of Tetracycline from Aqueous Solution, British Journal of Pharmaceutical Research 12(1) (2016) 1-11.

[48] L. Yi, L. Zuo, C. Wei, H. Fu, X. Qu, S. Zheng, Z. Xu, Y. Guo, H. Li, D. Zhu, Enhanced adsorption of bisphenol A, tylosin, and tetracycline from aqueous solution to nitrogen-doped multiwall carbon nanotubes via cation-pi and pi-pi electron-donor-acceptor (EDA) interactions, Sci Total Environ 719 (2020) 137389.

[49] W. Xiong, G. Zeng, Z. Yang, Y. Zhou, C. Zhang, M. Cheng, Y. Liu, L. Hu, J. Wan, C. Zhou, R. Xu, X. Li, Adsorption of tetracycline antibiotics from aqueous solutions on nanocomposite multi-walled carbon nanotube functionalized MIL-53(Fe) as new adsorbent, Sci Total Environ 627 (2018) 235-244.

[50] W.A. Khanday, B.H. Hameed, Zeolite-hydroxyapatite-activated oil palm ash composite for antibiotic tetracycline adsorption, Fuel 215 (2018) 499-505.

[51] E. Yeşilova, B. Osman, A. Kara, E. Tümay Özer, Molecularly imprinted particle embedded composite cryogel for selective tetracycline adsorption, Separation and Purification Technology 200 (2018) 155-163.

[52] W. Xiong, Z. Zeng, G. Zeng, Z. Yang, R. Xiao, X. Li, J. Cao, C. Zhou, H. Chen, M. Jia, Y. Yang, W. Wang, X. Tang, Metal-organic frameworks derived magnetic carbon-αFe/Fe3C composites as a highly

effective adsorbent for tetracycline removal from aqueous solution, Chemical Engineering Journal 374 (2019) 91-99.

[53] A.A. Edathil, I. Shittu, J. Hisham Zain, F. Banat, M.A. Haija, Novel magnetic coffee waste nanocomposite as effective bioadsorbent for Pb(II) removal from aqueous solutions, Journal of Environmental Chemical Engineering 6(2) (2018) 2390-2400.

[54] A.A. Oladipo, A.O. Ifebajo, Highly efficient magnetic chicken bone biochar for removal of tetracycline and fluorescent dye from wastewater: Two-stage adsorber analysis, J Environ Manage 209 (2018) 9-16.

[55] H.M. Jang, E. Kan, A novel hay-derived biochar for removal of tetracyclines in water, Bioresour Technol 274 (2019) 162-172.

[56] X. Zhu, Y. Liu, F. Qian, C. Zhou, S. Zhang, J. Chen, Preparation of magnetic porous carbon from waste hydrochar by simultaneous activation and magnetization for tetracycline removal, Bioresour Technol 154 (2014) 209-14.

[57] A. Behnamfard, M.M. Salarirad, Equilibrium and kinetic studies on free cyanide adsorption from aqueous solution by activated carbon, J Hazard Mater 170(1) (2009) 127-33.

[58] K.Y. Foo, B.H. Hameed, Insights into the modeling of adsorption isotherm systems, Chemical Engineering Journal 156(1) (2010) 2-10.

[59] S.J. Allen, G. McKay, J.F. Porter, Adsorption isotherm models for basic dye adsorption by peat in single and binary component systems, J Colloid Interface Sci 280(2) (2004) 322-33.

[60] A.S. Franca, L.S. Oliveira, M.E. Ferreira, Kinetics and equilibrium studies of methylene blue adsorption by spent coffee grounds, Desalination 249(1) (2009) 267-272.

[61] H.-T. Fan, L.-Q. Shi, H. Shen, X. Chen, K.-P. Xie, Equilibrium, isotherm, kinetic and thermodynamic studies for removal of tetracycline antibiotics by adsorption onto hazelnut shell derived activated carbons from aqueous media, RSC Advances 6(111) (2016) 109983-109991.

[62] Panhekar Deepa, B. Pooja, LANGMUIR_FREUNDLICH_TEMKIN_AND_DUBININ-RADUSHKEVICH ISOTHERM STUDIES OF EQUILIBRIUM SORPTION OF Pb（II）ONTO A.FICOIDEA, IJRAR 6(2) (2019) 698-704.

[63] K.L. Tan, B.H. Hameed, Insight into the adsorption kinetics models for the removal of contaminants from aqueous solutions, Journal of the Taiwan Institute of Chemical Engineers 74 (2017) 25-48.

[64] Z.H. Kheiralla, N.S. El-Gendy, H.A. Ahmed, T.H. Shaltout, M.M.D. Hussein, One-factor-at-a-time (OFAT) optimization of hemicellulases production from Fusarium moniliforme in submerged fermentation, Energy Sources, Part A: Recovery, Utilization, and Environmental Effects 40(15) (2018) 1877-1885.

[65] A.S. Abdulhameed, A.H. Jawad, A.T. Mohammad, Synthesis of chitosan-ethylene glycol diglycidyl ether/TiO2 nanoparticles for adsorption of reactive orange 16 dye using a response surface methodology approach, Bioresour Technol 293 (2019) 122071.

[66] T.V. Tran, D.T.C. Nguyen, H.T.N. Le, L.G. Bach, D.N. Vo, K.T. Lim, L.X. Nong, T.D. Nguyen, Combined Minimum-Run Resolution IV and Central Composite Design for Optimized Removal of the Tetracycline Drug Over Metal(-)Organic Framework-Templated Porous Carbon, Molecules 24(10) (2019).

[67] A. Khataee, B. Kayan, D. Kalderis, A. Karimi, S. Akay, M. Konsolakis, Ultrasound-assisted removal of Acid Red 17 using nanosized Fe3O4-loaded coffee waste hydrochar, Ultrason Sonochem 35(Pt A) (2017) 72-80.

[68] N. Subedi, A. Lahde, E. Abu-Danso, J. Iqbal, A. Bhatnagar, A comparative study of magnetic chitosan (Chi@Fe3O4) and graphene oxide modified magnetic chitosan (Chi@Fe3O4GO) nanocomposites for efficient removal of Cr(VI) from water, Int J Biol Macromol 137 (2019) 948-959.

[69] L.F. Ballesteros, J.A. Teixeira, S.I. Mussatto, Chemical, Functional, and Structural Properties of Spent Coffee Grounds and Coffee Silverskin, Food and Bioprocess Technology 7(12) (2014) 3493-3503.

[70] J. Majeed, K.C. Barick, N.G. Shetake, B.N. Pandey, P.A. Hassan, A.K. Tyagi, Water-dispersible polyphosphate-grafted Fe3O4 nanomagnets for cancer therapy, RSC Advances 5(105) (2015) 86754-86762.

[71] M. Foroughi, M.H. Ahmadi Azqhandi, S. Kakhki, Bio-inspired, high, and fast adsorption of tetracycline from aqueous media using Fe3O4-g-CN@PEI-beta-CD nanocomposite: Modeling by response surface methodology (RSM), boosted regression tree (BRT), and general regression neural network (GRNN), J Hazard Mater 388 (2020) 121769.

[72] S. Fan, Y. Wang, Y. Li, Z. Wang, Z. Xie, J. Tang, Removal of tetracycline from aqueous solution by biochar derived from rice straw, Environ Sci Pollut Res Int 25(29) (2018) 29529-29540.

[73] Z. Cheng, X. Liu, M. Han, W. Ma, Adsorption kinetic character of copper ions onto a modified chitosan transparent thin membrane from aqueous solution, J Hazard Mater 182(1-3) (2010) 408-15.

[74] F. Togue Kamga, Modeling adsorption mechanism of paraquat onto Ayous (Triplochiton scleroxylon) wood sawdust, Applied Water Science 9(1) (2018).

[75] Y. Li, S. Wang, Y. Zhang, R. Han, W. Wei, Enhanced tetracycline adsorption onto hydroxyapatite by Fe(III) incorporation, Journal of Molecular Liquids 247 (2017) 171-181.

[76] P. Liao, Z. Zhan, J. Dai, X. Wu, W. Zhang, K. Wang, S. Yuan, Adsorption of tetracycline and chloramphenicol in aqueous solutions by bamboo charcoal: A batch and fixed-bed column study, Chemical Engineering Journal 228 (2013) 496-505.

[77] M.A. Ahsan, S.K. Katla, M.T. Islam, J.A. Hernandez-Viezcas, L.M. Martinez, C.A. Díaz-Moreno, J. Lopez, S.R. Singamaneni, J. Banuelos, J. Gardea-Torresdey, J.C. Noveron, Adsorptive removal of methylene blue, tetracycline and Cr(VI) from water using sulfonated tea waste, Environmental Technology & Innovation 11 (2018) 23-40.

[78] A. Saldaña-Robles, R. Guerra-Sánchez, M.I. Maldonado-Rubio, J.M. Peralta-Hernández, Optimization of the operating parameters using RSM for the Fenton oxidation process and adsorption on vegetal carbon of MO solutions, Journal of Industrial and Engineering Chemistry 20(3) (2014) 848-857.